January 2026

FONDAZIONE ENI ENRICO MATTEI

Working Paper

02.2026

Industrial Metal Supply Shocks and Heterogeneous Macroeconomic Effects: Evidence from Copper

Andrea Bastianin, Luca Rossini, Alessandra Testa

Industrial Metal Supply Shocks and Heterogeneous Macroeconomic Effects: Evidence from Copper

Andrea Bastianin (University of Milan and Fondazione Eni Enrico Mattei), **Luca Rossini** (University of Milan and Fondazione Eni Enrico Mattei), **Alessandra Testa** (Fondazione Eni Enrico Mattei)

Summary

This paper studies the macroeconomic effects of global copper supply shocks. We identify exogenous disruptions to copper supply using a Bayesian structural VAR of the world copper market that combines sign and narrative restrictions. We then trace the international transmission of the identified shock using a two-step approach based on country-level models for major copper-importing and exporting economies. We find that copper supply shocks raise producer prices and depress industrial activity in importing economies, while exporters benefit from higher world prices through improved terms of trade. Importer-exporter status alone is insufficient to characterize exposure: heterogeneity in responses reflects differences in manufacturing copper intensity and buffering capacity through secondary copper production.

Keywords: Copper; Supply shocks; Structural VAR; Narrative identification; Macroeconomic effects.

JEL Classification: C32, E00, Q4

Corresponding Author
Andrea Bastianin
Università degli Studi di Milano
Dipartimento di Economia, Management e Metodi Quantitativi
Via Livorno, 1 - 20122 Milano
andrea.bastianin@unimi.it

Industrial Metal Supply Shocks and Heterogeneous Macroeconomic Effects: Evidence from Copper

Andrea Bastianin* Luca Rossini† Alessandra Testa ‡

January 12, 2026

Abstract: This paper studies the macroeconomic effects of global copper supply shocks. We identify exogenous disruptions to copper supply using a Bayesian structural VAR of the world copper market that combines sign and narrative restrictions. We then trace the international transmission of the identified shock using a two-step approach based on country-level models for major copper-importing and exporting economies. We find that copper supply shocks raise producer prices and depress industrial activity in importing economies, while exporters benefit from higher world prices through improved terms of trade. Importer-exporter status alone is insufficient to characterize exposure: heterogeneity in responses reflects differences in manufacturing copper intensity and buffering capacity through secondary copper production.

Key Words: Copper; Supply shocks; Structural VAR; Narrative identification; Macroeconomic effects.

JEL Codes: C32, E00, Q4

*University of Milan, Italy and Fondazione Eni Enrico Mattei (FEEM). andrea.bastianin@unimi.it
†University of Milan, Italy and Fondazione Eni Enrico Mattei (FEEM). luca.rossini@unimi.it
‡Fondazione Eni Enrico Mattei (FEEM) alessandra.testa@feem.it

1 Introduction

The macroeconomic consequences of commodity supply shocks have long been a central theme in the business-cycle literature, with most empirical evidence focusing on the oil market. Much less is known about the macroeconomic effects of supply disturbances in industrial metals, despite their growing importance for global production networks and the energy transition. Copper is a particularly relevant case: it is a widely used intermediate input and a critical material for electrification, renewable energy technologies, and, more recently, AI infrastructure, while its production is highly geographically concentrated. As a result, local disruptions – such as labor strikes or extreme weather events – can generate large and plausibly exogenous shifts in global copper supply and real prices.

This paper quantifies the macroeconomic effects of global copper supply shocks and examines how these shocks propagate across countries with heterogeneous exposure to copper markets. The key empirical challenge is to isolate supply-driven movements in copper prices from demand-driven fluctuations that co-move with global economic activity. We address this challenge by identifying a global copper supply shock within a structural Vector Autoregressive (VAR) model of the world copper market and then tracing its transmission to macroeconomic aggregates in major net-importing and net-exporting economies.

We focus on copper supply shocks for two reasons. First, copper production is concentrated in a small set of producing countries, so disruptions in a single major producer can have disproportionate global effects. Second, many supply disruptions are plausibly exogenous to contemporaneous macroeconomic conditions, unlike demand shocks that reflect broader movements in global industrial activity and are harder to disentangle from the outcomes of interest.

Our identification strategy builds on advances in the oil-market literature, which has developed structural VAR approaches to disentangle supply-, demand-, and expectations-driven shocks. Early contributions rely on zero restrictions (Kilian, 2009), while later work employs sign restrictions and elasticity-based identification (Baumeister and Hamilton, 2019; Kilian and Murphy, 2014). Subsequent studies further refine identification by combining sign and narrative information (Antolín-Díaz and Rubio-Ramírez, 2018; Caldara et al., 2019) or exploiting high-frequency price movements around policy announcements (Känzig, 2021). Despite this progress, evidence on the macroeconomic effects of metal supply shocks remains limited, particularly for copper, where supply adjustment is slow and the value chain spans mining, refining, and fabrication.

Building on these methodological foundations, recent work has extended structural approaches to industrial metals and critical raw materials central to the energy transition. Boer et al. (2024) use a structural VAR based on annual data and a combination of zero, sign, and narrative restrictions to identify metal-specific demand shocks, highlighting copper, nickel, cobalt, and lithium as potential bottlenecks. Similarly, Baumeister et al. (2022) investigate the structural drivers of copper and aluminum prices using sign restrictions and elasticity estimates. Complementary contributions examine forecasting performance (Bastianin et al., 2025), price connectedness among major metals (Bastianin et al., 2023), the interaction between critical mineral prices and geopolitical risk (Saadaoui et al., 2025), and the impact of energy transition policies on critical metal prices (Romani and Casoli, 2024).

This paper makes three contributions. First, we identify a global copper supply shock in a Bayesian structural VAR model of the world copper market that includes copper production, global real economic activity, the real price of copper, and copper inventories. Identification combines sign restrictions with narrative information derived from a systematic review of supply-disruption episodes reported in Dow Jones Factiva and tied to observable contractions in mine output. Second, we trace the macroeconomic transmission of this shock using a two-step empirical design: the shock is identified once at the global level and then embedded in parsimonious country-level models, preserving comparability across outcomes and countries without repeatedly re-identifying the shock on changing samples. Third, we document heterogeneous transmission patterns across net-importing and net-exporting economies and relate these differences to production structure and buffering capacity along the copper value chain.

Our results show that a negative copper supply shock raises producer prices and leads to a contraction in industrial production, consistent with higher intermediate-input costs and supply bottlenecks. In net-importing economies, external conditions deteriorate and real exchange rates depreciate as terms of trade worsen. In net-exporting economies, higher world copper prices strengthen external balances and can support activity through income effects, but the magnitude of these gains depends on domestic production linkages and the scope for substitution toward secondary inputs. Overall, the findings point to pronounced asymmetries in the international incidence of copper supply disruptions.

The remainder of the paper is organized as follows. Section 2 provides background on the global copper market. Section 3 describes the econometric framework, the data, and identification scheme. Section 4 presents the empirical results, while robustness checks are discussed in Section 5. Section 6 concludes.

2 Copper Market

Copper is a key input to the global economy, with widespread use across construction, manufacturing, transportation, and electronics. Its macroeconomic relevance has increased markedly with the transition toward low-carbon energy systems. Copper is an essential input in most clean energy technologies – including renewable power generation, electric vehicles, and electricity networks for transmission and storage – making it a critical material for electrification and decarbonisation. The rapid expansion of AI infrastructure has become an additional structural source of copper demand, as data centers and associated power-grid upgrades are highly copper-intensive, reinforcing the persistence of demand growth and the macroeconomic impact of supply constraints (Brousse, 2025). Reflecting these trends, the IEA's *Global Critical Minerals Outlook 2025* projects that, under the "Net-Zero Emissions (NZE) by 2050" scenario, global copper demand will increase by approximately 47.8% by 2040 (International Energy Agency, 2025). See Figure 1.

On the supply side, copper extraction and refining are geographically concentrated in a small number of countries.[1] In 2023, the largest exporters of copper ores and concentrates were Chile (25.4%), Peru (20.9%), and Indonesia (8.8%), while the main importers were China (60.7%), Japan (11.7%), and South Korea (5.17%). Trade in refined copper displays a similarly concentrated structure, with Chile, the Democratic Republic of the Congo, and

[1]Copper ore is primarily extracted from porphyry and sediment-hosted deposits. These geological resources are unevenly distributed and increasingly difficult to access, as many high-grade reserves have already been depleted. New projects therefore tend to involve lower ore grades, greater depths, and more challenging environmental conditions, raising both production costs and ecological risks.

Figure 1: Copper market scenario: 2024–2040.

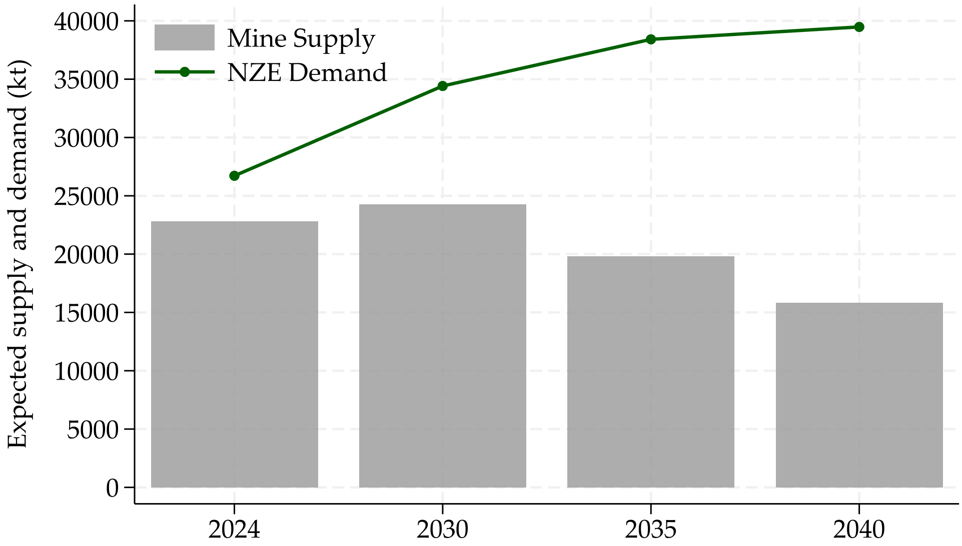

Notes: projected copper supply (gray bars) is constructed using data on operating and announced mining and refining projects by country. Projected demand under the IEA Net Zero Emissions by 2050 (NZE) scenario is shown by the green line. Authors' elaboration based on International Energy Agency (2025).

Japan accounting for a large share of global exports, and China and the United States dominating imports. This concentration implies that disruptions in a small set of producing countries can have disproportionate effects on global copper supply and prices.

Beyond concentration, copper supply is characterized by slow adjustment and high capital intensity. The supply chain spans multiple stages – from mining and concentrating to smelting, refining, and fabrication – each requiring specialised infrastructure and facing stringent environmental, social, and regulatory constraints. These frictions are most pronounced at the mining stage: new greenfield copper projects typically require around 17 years from discovery to commercial production, reflecting geological uncertainty, lengthy permitting processes, and financing risks (International Energy Agency, 2025). As a result, copper supply responds sluggishly to demand shocks and price signals.

Structural constraints on supply have intensified over time. Average copper ore grades have declined by around 40% since the early 1990s, substantially increasing capital intensity and operational complexity (International Energy Agency, 2025). In Latin America – the world's leading copper-producing region – average capital costs for brownfield projects have risen by approximately 65% since 2020 (International Energy Agency, 2025). At the same time, new resource discoveries have slowed sharply: of the 239 copper deposits identified globally between 1990 and 2023, only 14 were discovered in the past decade (International Energy Agency, 2025).

These structural features are reflected in the current investment pipeline. Despite substantial announced investments – requiring around 350 billion U.S. dollar in mining capital expenditure by 2040 – expected mine supply under existing policy settings falls short of projected demand by roughly 30% by 2035 (International Energy Agency, 2025). Figure 1 shows that this gap is expected to persist over time, reflecting the limited scope for rapid supply expansion. By 2040, expected mine supply of 15,836 kt would cover only about 40.1% of projected demand in the NZE scenario (39,480 kt), leaving a gap of 23,644 kt.

The combination of rapidly rising demand, geographic concentration, and slow supply adjustment creates a critical bottleneck in the global copper market, increasing vulnerability to supply-side shocks. Events such as labour strikes, extreme weather, regulatory interventions, or geopolitical tensions in a small number of producing countries can therefore generate large and sustained global effects on copper prices and downstream production costs. Recycling provides only limited short-term relief from these constraints. At present, recycled material accounts for roughly 18% of global copper demand, and scaling up secondary supply faces technical, economic, and institutional barriers (International Energy Agency, 2025). Consequently, primary supply conditions remain central in shaping copper market dynamics.

Taken together, these features imply that copper supply shocks are likely to be persistent, globally transmitted, and sizeable. Understanding their impact is therefore essential not only for major import-dependent economies – where copper is a key input for manufacturing, infrastructure investment, and the energy transition – but also for net-exporting economies, in which the mining sector plays a pivotal role.

3 Empirical strategy and data

The objective of this paper is to quantify the macroeconomic effects of global copper supply shocks and to trace their transmission across countries with heterogeneous exposure to copper markets. Our empirical strategy is structured in two steps. In the first step, we identify and estimate a global copper supply shock using a structural VAR model of the world copper market, combining sign restrictions with narrative information tied to well-documented exogenous supply disruptions. In the second step, we study the propagation of this identified shock to a broad set of macroeconomic and financial variables using parsimonious country-level models.

This two-step approach reflects two considerations. First, identification of a global copper supply shock requires modeling the joint dynamics of production, real economic activity, real prices and inventories at the global level. Second, once such a shock is identified, its macroeconomic transmission can be analyzed separately without repeatedly re-estimating the shock, thereby ensuring consistency and comparability across countries, variables, and specifications.

3.1 A structural VAR model of the global copper marked

We model the global copper market using an n-variable structural VAR of order p,

$$\boldsymbol{A}_0 \boldsymbol{y}_t = \sum_{j=1}^{p} \boldsymbol{A}_j \boldsymbol{y}_{t-j} + \boldsymbol{v}_t, \qquad t = 1, \ldots, T, \tag{1}$$

where $\boldsymbol{y}_t$ is a (4×1) vector that includes global copper production, world industrial production, the real price of copper, and copper inventories. The vector $\boldsymbol{v}_t$ collects mutually orthogonal structural shocks, normalized such that $E(\boldsymbol{v}_t \boldsymbol{v}_t') = \boldsymbol{I}_n$. The corresponding reduced-form innovations are given by $\boldsymbol{\epsilon}_t = \boldsymbol{A}_0^{-1} \boldsymbol{v}_t$, with covariance matrix $\boldsymbol{\Sigma} = E(\boldsymbol{\epsilon}_t \boldsymbol{\epsilon}_t') = \boldsymbol{A}_0^{-1} \boldsymbol{A}_0^{-1'}$, where $\boldsymbol{A}_0^{-1}$ denotes the contemporaneous impact-response matrix. Further details are provided in the Supplement.

Identification of the copper supply shock requires restrictions on $\boldsymbol{A}_0^{-1}$. Rather than relying on a recursive ordering or a single exclusion restriction, we adopt a set-identification approach that combines sign restrictions with narrative information, following Antolín-Díaz and Rubio-Ramírez (2018). This choice is motivated by the nature of commodity markets, where point identification based on timing assumptions is often difficult to defend (Baumeister and Hamilton, 2019).

The combination of sign and narrative restrictions substantially narrows the admissible set of structural parameters, while preserving robustness to model misspecification and avoiding implausible zero restrictions. Importantly, the model remains set-identified.

3.1.1 Identification of the copper supply shock

To identify the copper supply shock, we combine sign restrictions on the impact response matrix $\boldsymbol{A}_0^{-1}$ with narrative information that constrains the sign of the structural shocks $\boldsymbol{v}_t$ around key historical events. Both sets of restrictions are summarized in Table 1.

Sign restrictions. We first impose standard sign restrictions consistent with a negative copper supply shock in panel (a) of Table 1: on impact, global copper production falls, the real price of copper rises, and refined copper inventories decline, while world industrial production is not allowed to increase contemporaneously. Taken alone, these restrictions typically yield a very large identified set, reflecting the fact that multiple structural representations can be consistent with the same reduced-form dynamics.

Narrative restrictions. To sharpen identification, we augment the sign-restriction framework with narrative restrictions tied to well-documented historical episodes widely regarded as exogenous disruptions to copper supply. These narrative restrictions constrain the sign of the identified structural shocks $\boldsymbol{v}_t$ during specific months associated with major supply-side events, ensuring that the recovered shock aligns with observable reductions in copper production.

To identify these events, we use Dow Jones Factiva, a comprehensive database of news articles. We focus on reports associated with disruptions in copper supply, defined as negative events linked to reductions in copper ore production. We first collect English-language articles containing references to copper alongside keywords such as "strikes", "disasters", "floods", and "water shortages". We then manually review these articles to isolate events that plausibly resulted in actual supply disruptions. This second step is essential, as some reported local events have negligible or no effects on global production. Panel (b) of Table 1 lists the four events that had a quantitatively meaningful impact on global copper mine production growth. All four events occurred in Chile, the world's largest copper producer, which accounted for an average of 30.1% of global copper mine output over the 1995–2024 period.

The labor strikes of August 2006 and February 2017 are associated with clear declines

Table 1: Sign and narrative restrictions.

(*a*) Sign restrictions				
	Production	WIP	Price	Inventories
Supply shock	-	-	+	-
(*b*) Narrative restrictions on copper production				
Date	Sign	Country	Event	% y/y
08-2006	Negative	Chile	Strike	-5.71 (-2.28)
02-2015	Negative	Chile	Flood	-17.56 (-11.01)
02-2017	Negative	Chile	Strike	-12.33 (-3.48)
08-2021	Negative	Chile	Drought	-3.37 (0.34)

Notes: In panel (*b*), column (5), "% y/y" reports the 12-month log growth rate of Chilean copper mine production (world copper ore production in brackets). Production data are sourced from the World Bureau of Metal Statistics.

in both Chilean and global copper production, with year-on-year growth rates of -5.71% and -12.33%, respectively, as highlighted in column 5 of Table 1(*b*). Weather-related disruptions have become increasingly frequent. Among these, water scarcity and droughts are particularly critical for copper mining, as extraction and ore processing are highly water-intensive. The February 2015 event corresponds to severe flooding that disrupted access to major mining sites, leading to an even sharper contraction in output (-17.56%). Finally, the August 2021 episode reflects drought-related water shortages that constrained mining and ore-processing operations, resulting in a production decline of -3.37%. Although the August 2021 drought event did not contemporaneously affect world copper production, global output declined persistently in the subsequent months, reaching a local minimum of -0.13% in November 2021, consistent with a delayed response of global copper supply.

3.2 Analysis of propagation channels

In the second step, we study how the identified global copper supply shock propagates to macroeconomic and financial variables at the country level. Rather than augmenting the global VAR with additional variables one at a time – which would require re-identifying the shock for each specification and would severely restrict the usable sample – we adopt a two-step approach inspired by Kilian (2009), Kilian et al. (2009), and Forni et al. (2024), among others.

Specifically, we treat the estimated copper supply shock as an observed external shock and embed it in a sequence of bivariate structural VAR models estimated separately for each country and outcome variable. In each bivariate system, the copper supply shock is ordered first and the country-specific variable second, ensuring contemporaneous exogeneity of the global shock. This design isolates the dynamic response of each variable to a common global disturbance while keeping the identified shock fixed across specifications, thereby facilitating meaningful cross-country and cross-variable comparisons. Importantly the bivariate VARs are not intended to re-identify the global supply shock, but solely to trace its dynamic transmission.

While a larger multivariate VAR would be preferable in principle (Känzig, 2021), data limitations across countries and variables would require changing samples and repeatedly re-identifying the shock, thereby undermining comparability across specifications. The bivariate SVAR approach therefore represents a pragmatic compromise: it preserves a consistent shock measure across exercises, limits overfitting, and allows us to trace heterogeneous transmission patterns across countries and channels.[2]

Overall, this empirical strategy provides a transparent and flexible analysis of macroeconomic propagation, while explicitly accounting for identification uncertainty and data limitations.

3.3 Data and country selection

The structural VAR model for the global copper market includes four monthly variables: the growth rate of global copper mine production, an index of real economic activity, the log of the real price of copper, and the growth rate of refined copper inventories. All series are available from January 1994 to December 2024.[3]

Global copper mine production and refined copper inventories data are obtained from the World Bureau of Metal Statistics.[4] The three-month futures price of copper on the London Metal Exchange (LME), quoted in U.S. dollars per metric ton, is sourced from Refinitiv and deflated using the U.S. CPI. As a measure of global real economic activity, we use the

[2] An alternative approach would be to use local projections (LPs) with the identified shock as a regressor. We analyse LP-based impulse responses in Section 5. See Ho et al. (2024) for evidence that VAR- and LP-based impulse responses can be complementary under model misspecification and Montiel Olea et al. (2025) for a broader comparison of LP and VAR models.

[3] A more detailed description of the dataset is provided in the Supplement.

[4] Since production data exhibit seasonality, we deseasonalise the series using month-of-the-year dummy variables.

Table 2: Copper trade by country and stage of production, avg. 1995–2024 (Mt).

	Chile	Japan	Mexico	USA
(*a*) Ores and concentrates				
Export Quantity	2.373	0.000	0.672	0.195
Import Quantity	0.050	4.665	0.165	0.044
Trade Balance	2.323	-4.665	0.507	0.151
(*b*) Refined copper				
Export Quantity	2.251	0.449	0.055	0.133
Import Quantity	0.001	0.104	0.047	0.701
Trade Balance	2.250	0.345	0.008	-0.568
(*c*) Total				
Export Quantity	4.623	0.450	0.727	0.328
Import Quantity	0.050	4.769	0.211	0.745
Trade Balance	4.573	-4.319	0.516	-0.417

Notes: authors' calculations based on UN Comtrade data for copper ores and concentrates (HS 2603) and refined copper (HS 7403). The table reports period averages for 1995-2024. All quantities are expressed in megatonnes (Mt).

monthly world industrial production (WIP) index constructed by Baumeister and Hamilton (2019).

In the second step of the analysis, we consider a set of macroeconomic variables for selected copper-importing and copper-exporting economies. These include producer price indices and industrial production indices across various sectors, real effective exchange rates, and terms of trade. The sample period extends from December 1995 to December 2024.

The selection of countries included in the analysis reflects a trade-off between data availability and the representativeness of the sample. To balance these objectives, we focus on four economies that occupy distinct positions along the global copper value chain: two net importers, the United States and Japan, and two net exporters, Chile and Mexico.

Table 2 shows that the role of countries changes across stages of production. The United States and Mexico are net exporters of copper ores and concentrates, but their positions differ downstream: the United States is a sizable net importer of refined copper (-0.57 Mt), whereas Mexico's refined trade is approximately balanced. Japan displays the opposite pattern, acting as a large net importer of ores (-4.67 Mt) and a net exporter of refined copper (0.35 Mt), consistent with its role as a downstream processing hub. Chile is the only country that is a net exporter at both stages, with large surpluses in ores and refined copper.

When trade flows are aggregated across stages, a clearer classification emerges. Over

1995–2024, the United States and Japan exhibit negative overall copper trade balances, while Chile and Mexico record positive balances. This integrated perspective is particularly relevant for analysing global supply-side shocks, which originate upstream but propagate through prices along the entire value chain, ultimately affecting refined copper prices faced by downstream users.[5]

4 Results

4.1 Copper supply shocks

We begin by presenting results from a structural VAR model of the global copper market. Based on the Akaike information criterion, we select a lag order of p=10 and estimate the model using monthly data from January 1994 to December 2024.[6] The model is estimated within a Bayesian framework, employing a Minnesota prior on the reduced-form VAR parameters.

Our identification strategy delivers a set-identified copper supply shock: rather than a single point estimate, the procedure yields 1,000 admissible posterior draws that satisfy the imposed identifying restrictions.

Supply shocks. Figure 2 displays the copper supply shock identified using sign and narrative restrictions, aggregated to quarterly frequency for ease of visualization. Since the shock is set-identified, the figure reports the median across the 1,000 posterior draws that satisfy the identifying restrictions. The gray shaded areas indicate major exogenous events that affected the copper market. Consistent with the evidence reported in Table 1, the estimated global supply shock exhibits large negative spikes coinciding with the narrative events. Although these events originate at the local level, they are associated with clear and economically meaningful contractions in global copper supply.

Forecast error variance decomposition. To assess the quantitative importance of copper supply shocks, we report the forecast error variance decomposition (FEVD) of the real

[5] At the same time, this integrated perspective has limitations, as aggregation across stages may mask important asymmetries in adjustment mechanisms between mining and refining.

[6] The results are robust to specifications with 12 lags, a conventional choice for monthly data (see Supplement). Most computations are performed using the *Empirical Macro Toolbox* of Ferroni and Canova (2025).

Figure 2: Copper supply shock aggregated at quarterly frequency.

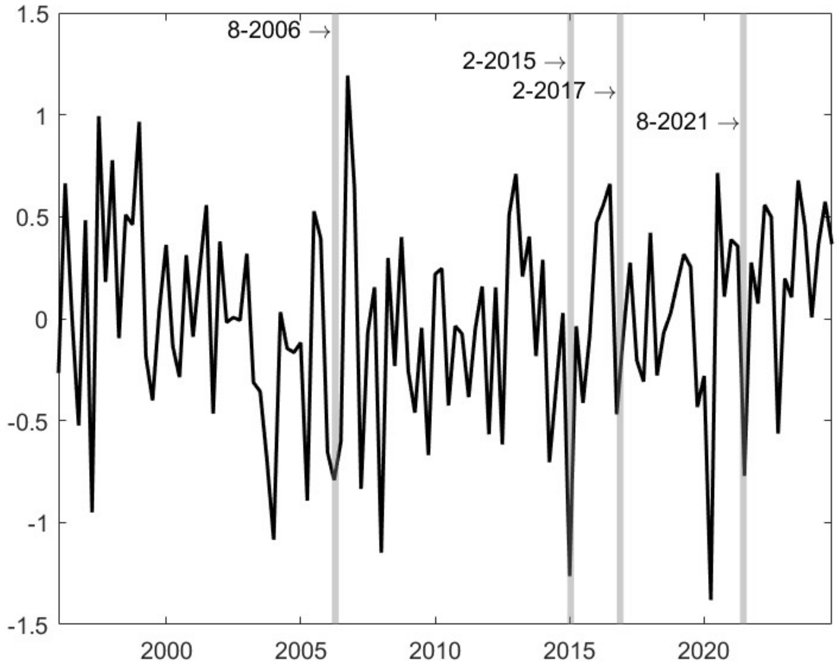

Notes: copper supply shock aggregated at quarterly frequency (black line). The gray bands correspond to the four narrative events used for identification.

price of copper. The FEVD measures the share of forecast error variance in copper price fluctuations attributable to supply shocks and to other structural disturbances. Since the model is set-identified, the FEVD is computed for each admissible posterior draw and then averaged across the 1,000 draws that satisfy the identifying restrictions.

On impact, copper supply shocks account for approximately 22.9% of real copper price fluctuations. Their contribution gradually declines over time, reaching about 17.4% after two years. As only one structural shock is identified, the remaining variation in copper prices reflects the combined influence of other shocks, including aggregate demand and expectations-driven innovations. These magnitudes indicate that copper supply conditions play a quantitatively important role in price formation, consistent with a structurally tight market in which supply disruptions translate into sizable and persistent price movements.[7]

Impulse-response analysis. Figure 3 reports the structural impulse response functions (IRFs) of the four global copper market variables to a negative copper supply shock, over a horizon

[7] In the Supplement we report the historical decomposition of the real price of copper.

Figure 3: IRFs to the negative copper supply shock.

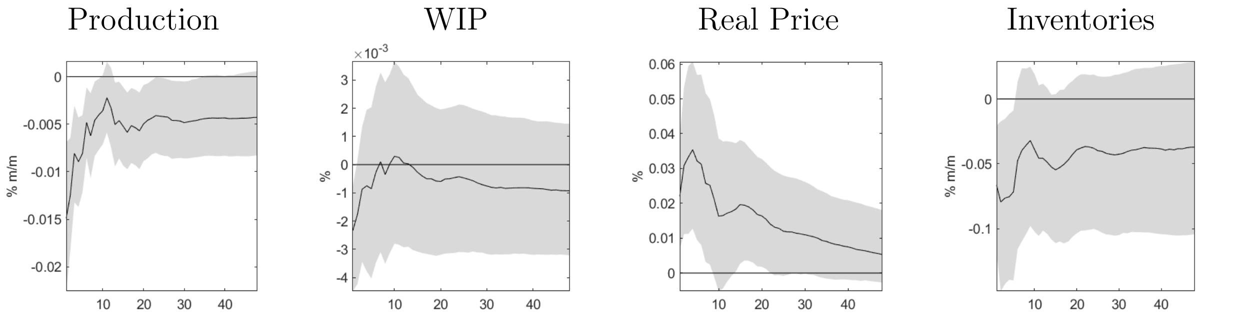

Notes: IRFs are based on 1,000 draws. The black solid line shows the median response, the gray shaded area represents the 68% pointwise credible set.

of four years (48 months). Following Antolín-Díaz and Rubio-Ramírez (2018), we summarize the IRFs using the pointwise median across admissible draws (black line) and report 68% credible bands (gray area).[8]

Figure 3 shows that global copper production declines sharply and persistently following a negative supply shock. The real price of copper increases on impact, peaks after approximately three months, and then gradually declines as the effect dissipates. World industrial production (WIP) also falls on impact but recovers relatively quickly, consistent with a temporary slowdown in global manufacturing driven by higher input costs. Finally, copper inventories exhibit a modest and short-lived decline immediately after the shock, suggesting a brief drawdown of existing stocks in response to the production disruption. Overall, these responses are consistent with the evidence in Boer et al. (2023) and, more generally, with established findings from the oil-market literature.

4.2 The macroeconomic effects of copper supply shocks

Global disruptions in the supply of copper can have significant macroeconomic impacts for economies that rely heavily on imported copper. For net-importing countries, a negative supply shock primarily operates through two main channels: a price channel, whereby higher copper prices feed into producer prices and production costs, and a real-external channel, as higher input costs and changes in trade values affect industrial activity, the trade balance,

[8]Pointwise summaries of IRFs provide only a partial characterization of the set of admissible dynamics and may underestimate uncertainty by ignoring dependence across horizons and variables (Inoue and Kilian, 2022). We adopt this convention for ease of exposition and comparability with the literature, and verify in robustness checks that our qualitative results are robust when examining the full set of admissible IRFs.

Table 3: Structural indicators for copper supply shock transmission: 2017-2019.

	Chile	Japan	Mexico	United States
Copper intensity of GDP (kg per mn USD, 2010)	0.13	4.87	112.70	41.89
Copper intensity of manufacturing VA (kg per mn USD, 2010)	1.41	23.82	561.49	373.06
Manufacturing share of GVA (%)	10.28	20.53	21.25	11.65
Secondary copper share (%)	–	38.90	8.70	2.30

Notes: Copper intensity is measured as kilograms of refined copper imports per million USD of real GDP or manufacturing value added (2010 prices). The secondary copper share is defined as secondary (scrap-based) refined copper production relative to country refined copper consumption. Figures are averaged over 2017–2020. Authors' calculations based on WBMS and World Bank data. Chile reports no secondary refined copper production in this period.

and the real effective exchange rate (REER). The strength and timing of these effects depend on structural characteristics such as copper intensity, the degree of cost pass-through, and the scope for substitution or inventory adjustment.

Table 3 highlights substantial cross-country heterogeneity in exposure to copper supply shocks. Copper intensity measured at the level of manufacturing value added (VA) is an order of magnitude larger than at the aggregate GDP level in all countries, underscoring the central role of industrial production in transmitting supply disruptions. Among net importers, the United States exhibits markedly higher copper intensity in manufacturing than Japan, which is suggestive of relatively stronger cost pressures on industrial activity following a supply shock. By contrast, Japan's higher manufacturing share in gross value added (GVA) provides suggestive evidence that copper price increases may be more likely to pass through to producer prices.

Differences in buffering capacity – proxied by the share of secondary (scrap-based) copper in total refined consumption – may further influence the persistence of supply shocks. Japan's relatively high secondary copper share is suggestive of greater scope for substitution toward recycled inputs, which may attenuate real-side effects. By contrast, the more limited use of secondary copper in the United States points to potentially tighter short-run constraints.

Among exporters, Chile's negligible import-based copper intensity and limited role of secondary production are suggestive of a transmission of supply shocks operating primarily through export prices and revenues. By contrast, Mexico's higher copper intensity and more limited buffering capacity provide suggestive evidence that production linkages may amplify real effects, despite its exporter status.

Taken together, these structural differences are consistent with a role for both trade position and production structure in shaping the cross-country propagation of copper supply shocks.

4.3 Impulse response analysis for net-importers and net-exporters

We present IRFs of selected macroeconomic variables to a negative (median) copper supply shock identified in Section 4.1. Country-level bivariate VAR models are estimated by OLS with six lags using monthly data from January 1995 to December 2024. All IRFs are normalized to a one–standard deviation copper supply shock. Solid black lines denote point estimates, while shaded gray areas indicate 68 percent confidence bands constructed from 5,000 bootstrap replications.[9]

4.3.1 The impact of copper supply shocks for net-importers

The United States and Japan occupy predominantly downstream positions in the global copper value chain, but with distinct roles. In 2023, the United States accounted for a small share of global refined copper exports (1.04%) while importing a non-negligible share of refined copper, implying that its exposure to copper supply disruptions operates mainly through higher refined copper prices and cost pass-through. Japan, by contrast, functions as a downstream processing hub, absorbing 11.7% of global copper ore imports while exporting 7.35% of refined copper, making it particularly exposed to disruptions in input sourcing and downstream processing costs.[10]

United States. Figure 4 reports the macroeconomic responses of the United States to a negative copper supply shock. Producer prices increase persistently across sectors, with particularly strong effects in manufacturing and mining. This pattern is consistent with a cost-push mechanism, whereby higher copper prices are transmitted along the production chain and raise input costs in copper-intensive industries.

[9]Bootstrap confidence bands are obtained by resampling initial conditions and least-squares residuals. Results are robust to specifications with 12 lags; see the Supplement.

[10]These data are sourced from the Observatory of Economic Complexity (Simoes and Hidalgo, 2011).

Figure 4: IRFs for the United States.

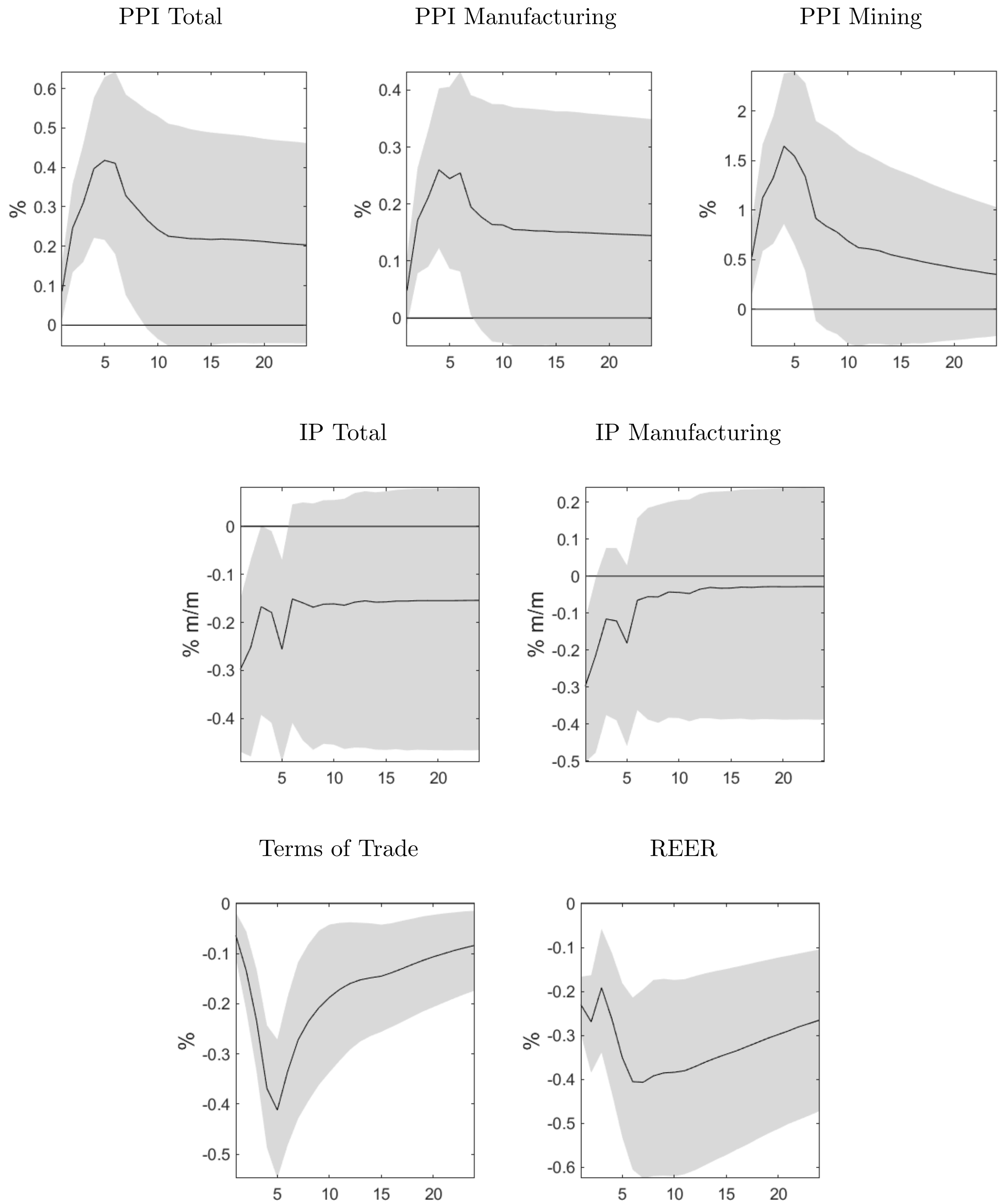

Notes: gray shaded areas represent 68% confidence bands based on 5,000 bootstrap replications. In all specifications, the response variable is expressed as 100 times the logarithm of the underlying series. The sole exception is IP, which enters the model in 100 times log differences; for these specifications, impulse responses are reported in cumulated form.

Industrial production declines on impact, especially in manufacturing, reflecting the importance of copper as an intermediate input. As shown in Table 3, U.S. manufacturing is highly copper-intensive, which amplifies the real effects of supply disruptions despite the relatively modest share of manufacturing in aggregate value added. Moreover, the low secondary copper share points to limited scope for substitution toward recycled inputs, contributing to tighter short-run production constraints.

On the external side, the real effective exchange rate depreciates and the terms of trade deteriorate, consistent with higher import prices. Taken together, the U.S. responses are characteristic of a copper-importing economy in which strong manufacturing linkages and limited buffering capacity magnify the impact of global supply disruptions.

Figure 5: IRFs for Japan.

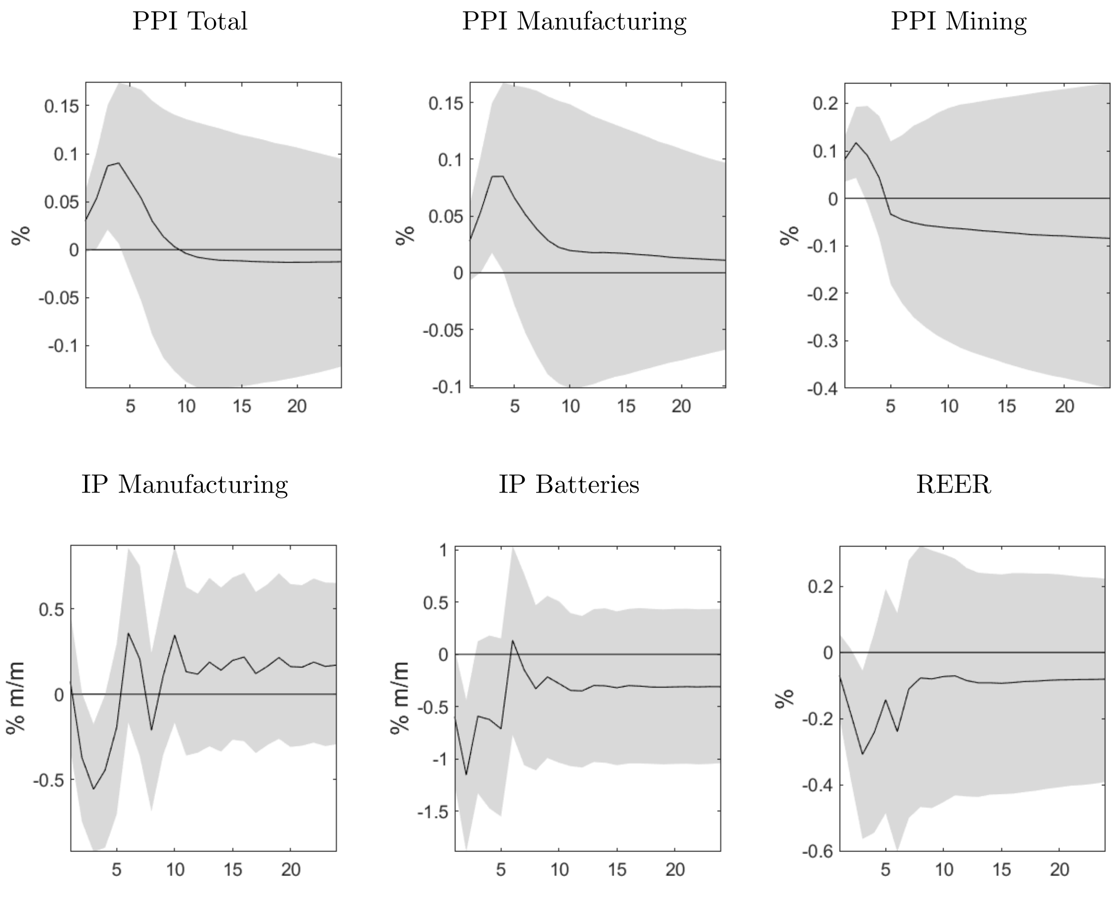

Notes: see notes to Figure 4.

Japan. Figure 5 reports the responses for Japan. Producer prices exhibit only a mild and short-lived increase following the copper supply shock, and the effects are generally not statistically significant. This muted price response contrasts with the United States and points to limited cost pass-through into domestic prices.

Industrial production nonetheless declines on impact, particularly in the battery-related sector, before recovering relatively quickly. As shown in Table 3, Japan combines moderate copper intensity in manufacturing with a high manufacturing share in gross value added, implying exposure to input cost shocks. At the same time, Japan exhibits a very high secondary copper share, which provides greater scope for substitution toward recycled inputs. This buffering capacity helps explain the short-lived real effects and the faster normalization of activity.

Consistent with these dynamics, the real effective exchange rate depreciates persistently, reflecting a deterioration in external conditions for a small open economy facing an adverse terms-of-trade shock. Taken together, Japan's responses highlight the role of substitution capacity in mitigating the persistence of copper supply shocks.

4.3.2 The impact of copper supply shocks for net-exporters

We next examine the macroeconomic effects of copper supply shocks in net-exporting economies, focusing on Chile and Mexico, which represent two distinct forms of upstream exposure along the copper value chain. Chile occupies a clearly upstream position, accounting in 2023 for 25.4% of global copper ore exports and 19.7% of refined copper exports, with negligible import shares. This implies that copper supply shocks should transmit primarily through export prices and income effects. Mexico, by contrast, holds an intermediate position along the value chain, combining a non-trivial share of copper ore exports (3.46%) with a more balanced refined copper trade. As a result, supply shocks in Mexico are expected to propagate through both price and real production channels rather than solely through export revenues. Although both countries record positive overall copper trade balances (see Table 2), their structural characteristics differ markedly, leading to heterogeneous macroeconomic responses.

Chile. As we can see from the top panels of Figure 6, following a negative copper supply shock, industrial production increases on impact and remains positive in the short run, consistent with higher export revenues driven by rising copper prices. As shown in Table

Figure 6: IRFs for Chile and Mexico.

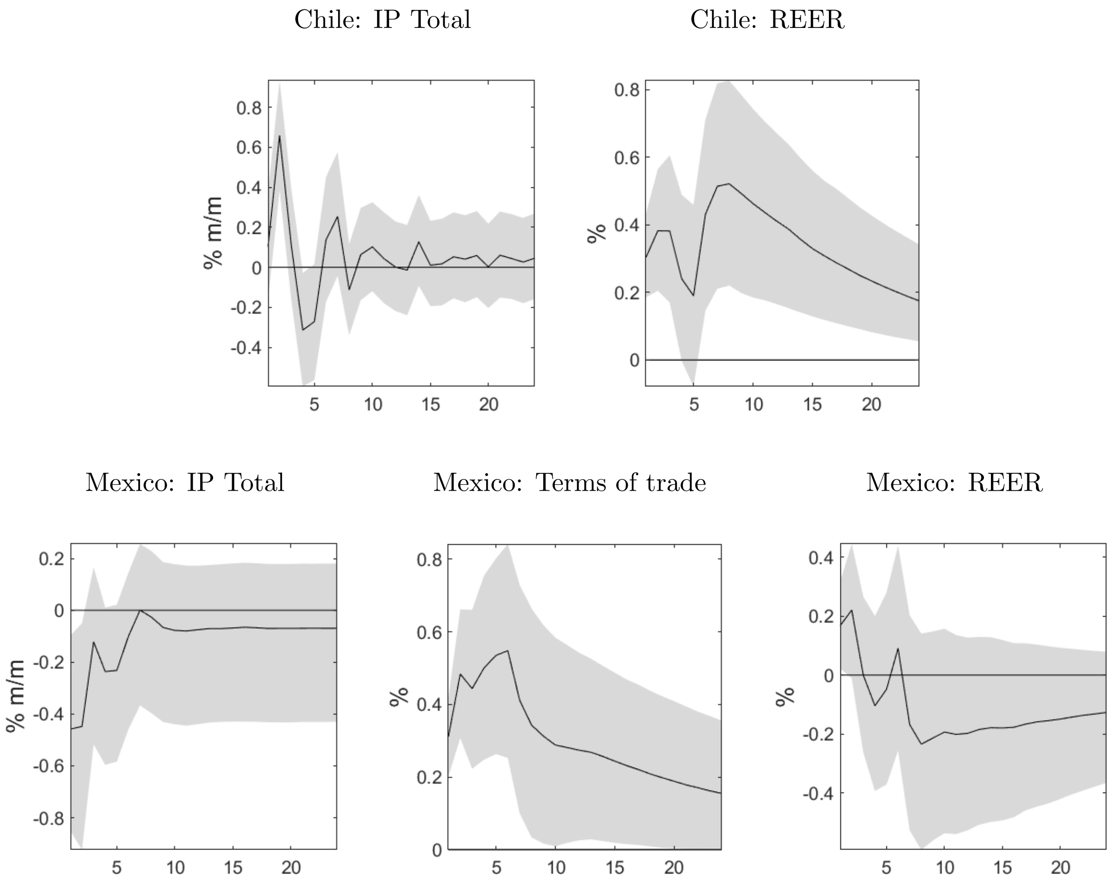

Notes: see notes to Figure 4.

3, Chile has negligible import-based copper intensity and no secondary refined copper production, implying that domestic production costs are largely insulated from higher copper prices. Consequently, the transmission of the shock operates primarily through export-price and income channels. The real effective exchange rate appreciates significantly on impact, reflecting improved external conditions, before gradually reverting toward baseline.

Mexico. The bottom panels of Figure 6 show the responses for Mexico. In this case, although the real effective exchange rate appreciates and the terms of trade improve on impact, industrial production declines initially and recovers only gradually. This pattern is consistent with Mexico's very high copper intensity in manufacturing and limited secondary copper share (see Table 3), which imply strong production linkages and limited buffering capacity. Consequently, despite its exporter status, copper supply shocks generate non-negligible real-side effects in Mexico.

Summary of results. Overall, our results indicate that exporter or importer status alone is insufficient to characterize the macroeconomic impact of copper supply shocks. Instead, transmission depends jointly on trade position, production structure, and buffering capacity. Net-importing economies are primarily affected through higher input costs and external adjustment, but the magnitude and persistence of these effects vary with copper intensity in manufacturing and the scope for substitution toward secondary inputs. Among exporters, positive price and income effects dominate only when domestic production is insulated from copper cost pressures, as in Chile, whereas strong production linkages and limited buffering capacity, as in Mexico, generate non-negligible real-side effects despite exporter status. These structural differences account for both the size and persistence of the heterogeneous macroeconomic responses observed across countries and are consistent with the mechanism identified by Fernández et al. (2017).

5 Robustness Checks

In this section we briefly illustrate a series of robustness checks, related to both the first and second stage of our analysis. More details are reported in the Supplement.

5.1 Alternative Structural VAR models

Dropping narrative restrictions. We re-estimate the structural VAR by jointly identifying a full set of structural shocks – including supply, economic activity, contemporaneous demand, and expectational demand shocks – using sign restrictions only by following Boer et al. (2024). Although this alternative specification does not rely on narrative information, the resulting copper supply shock closely mirrors the baseline shock in both timing and magnitude, and the associated impulse responses are robust in sign and broadly comparable in size.

Refined copper production. As an additional robustness check, we estimate an alternative structural VAR specification that explicitly includes refined copper production alongside mine production. While refined production responds negatively to a mining-driven supply shock, the effect is not statistically significant, reflecting lags in the copper production chain. The resulting impulse responses for prices, activity, and inventories remain qualitatively consistent with the baseline specification.

5.2 Second-stage sensitivity checks

We assess the robustness of our results along two dimensions. First, we re-estimate the second-step bivariate SVAR using multiple admissible draws of the set-identified copper supply shock obtained in the first stage. The corresponding impulse responses trace paths that broadly mirror the shape of the 68% confidence set based on the median supply shock.

Second, we compare our baseline SVAR impulse responses with those obtained from local projections (LPs). Specifically, for each horizon $h = 0, \ldots, 24$, we estimate LP impulse responses by regressing y_{t+h} on the identified (median) copper supply shock, controlling for lags of the variables, and computing HAC (Newey–West) standard errors.

Consistent with recent evidence on the relative performance of VARs and local projections (Montiel Olea et al., 2025), the LP IRFs exhibit greater sampling variability relative to the SVAR-based IRFs, especially at longer horizons, but deliver qualitatively comparable dynamic patterns. Taken together, these robustness exercises suggest that our main conclusions are not materially affected by the choice of shock draw or by the dynamic estimation framework.

6 Conclusion

This paper studies the macroeconomic effects of exogenous disruptions in global copper production, a topic that has received comparatively little attention despite copper's growing importance for industrial activity, the energy transition, and AI-related infrastructure. Using a Bayesian structural VAR, we identify global copper supply shocks with sign and narrative restrictions and document their effects on copper production, prices, global activity, and inventories. We then trace their international transmission using country-level bivariate SVARs for major net importers and exporters.

We find that copper supply disruptions behave as adverse supply shocks for net-importing economies: producer prices rise and industrial production contracts, consistent with cost-push pressures and input bottlenecks. Importers also experience a deterioration in external conditions, reflected in weaker terms of trade and real exchange-rate depreciation. In net-exporting economies, higher world copper prices tend to improve external balances and can support activity through income effects, but these gains are heterogeneous and depend on domestic production linkages.

A key implication of our evidence is that importer versus exporter status is not sufficient to characterize exposure. The cross-country responses are shaped by structural features along the copper value chain, including copper intensity in manufacturing and buffering capacity through secondary (scrap-based) copper. These mechanisms help rationalize why some exporters display non-negligible real-side effects, while some importers experience more muted and short-lived responses.

More broadly, our results complement the commodity-shock literature by showing that industrial metals can generate sizable and heterogeneous macroeconomic effects through both price and real-activity channels. Given the concentration of global copper supply and the slow pace of supply adjustment, monitoring supply vulnerabilities – and the role of recycling and other buffering margins – is important for assessing macroeconomic risks from future copper supply disruptions.

References

Antolín-Díaz, J. and J. F. Rubio-Ramírez (2018). Narrative sign restrictions for SVARs. *American Economic Review 108*(10), 2802–2829.

Bastianin, A., C. Casoli, and M. Galeotti (2023). The connectedness of energy transition metals. *Energy Economics 128*, 107183.

Bastianin, A., L. Rossini, and L. Tonni (2025). A real-time framework for forecasting metal prices. Nota di Lavoro 34.2025, Fondazione Eni Enrico Mattei.

Baumeister, C. and J. D. Hamilton (2019). Structural interpretation of vector autoregressions with incomplete identification: Revisiting the role of oil supply and demand shocks. *American Economic Review 109*(5), 1873–1910.

Baumeister, C., G. Verduzco-Bustos, and F. Ohnsorge (2022). Pandemic, war, recession:

Drivers of aluminum and copper prices. World Bank Commodity Markets Outlook. Special Focus.

Boer, L., A. Pescatori, and M. Stuermer (2023). Not all energy transitions are alike: disentangling the effects of demand and supply-side policies on future oil prices. IMF Working Paper 160, International Monetary Fund.

Boer, L., A. Pescatori, and M. Stuermer (2024). Energy transition metals: Bottleneck for net-zero emissions? *Journal of the European Economic Association 22*(1), 200–229.

Brousse, C. (2025, April). AI and the growth of data centres: challenges for the copper market. Banque de France, Eco Notepad No. 401. Published April 18, 2025.

Caldara, D., M. Cavallo, and M. Iacoviello (2019). Oil price elasticities and oil price fluctuations. *Journal of Monetary Economics 103*, 1–20.

Fernández, A., S. Schmitt-Grohé, and M. Uribe (2017). World shocks, world prices, and business cycles: An empirical investigation. *Journal of International Economics 108*(S1), S2–S14.

Ferroni, F. and F. Canova (2025). Empirical macro toolbox. Available online at: `https://github.com/naffe15/BVAR_`.

Forni, M., L. Gambetti, N. Maffei-Faccioli, and L. Sala (2024). Nonlinear transmission of financial shocks: Some new evidence. *Journal of Money, Credit and Banking 56*(1), 5–33.

Ho, P., T. A. Lubik, and C. Matthes (2024). Averaging impulse responses using prediction pools. *Journal of Monetary Economics 146*, 103571.

Inoue, A. and L. Kilian (2022). Joint Bayesian inference about impulse responses in VAR models. *Journal of Econometrics 231*(2), 457–476.

International Energy Agency (2025). Global critical minerals outlook 2025. International Energy Agency, Paris. `https://www.iea.org/reports/copper-2`.

Känzig, D. R. (2021). The macroeconomic effects of oil supply news: Evidence from OPEC announcements. *American Economic Review 111*(4), 1092–1125.

Kilian, L. (2009). Not all oil price shocks are alike: Disentangling demand and supply shocks in the crude oil market. *American Economic Review 99*(3), 1053–1069.

Kilian, L. and D. P. Murphy (2014). The role of inventories and speculative trading in the global market for crude oil. *Journal of Applied Econometrics 29*(3), 454–478.

Kilian, L., A. Rebucci, and N. Spatafora (2009). Oil shocks and external balances. *Journal of International Economics 77*(2), 181–194.

Montiel Olea, J. L., M. Plagborg-Møller, E. Qian, and C. K. Wolf (2025). Local Projections or VARs? A Primer for Macroeconomists. In J. V. Leahy and V. A. Ramey (Eds.), *NBER Macroeconomics Annual 2025*, Volume 40. University of Chicago Press.

Romani, I. G. and C. Casoli (2024). Understanding the future of critical raw materials for the energy transition: SVAR models for the US market. Working Paper 2024-05, MIT-CEEPR.

Saadaoui, J., R. Smyth, and J. Vespignani (2025). Ensuring the security of the clean energy transition: Examining the impact of geopolitical risk on the price of critical minerals. *Energy Economics 142*, 108195.

Simoes, A. J. G. and C. A. Hidalgo (2011). The economic complexity observatory: An analytical tool for understanding the dynamics of economic development. Workshops at the Twenty-Fifth AAAI Conference on Artificial Intelligence. Available online at: `https://oec.world/en`.

Supplement to *Industrial Metal Supply Shocks and Heterogeneous Macroeconomic Effects: Evidence from Copper*

Andrea Bastianin

University of Milan, Italy and Fondazione Eni Enrico Mattei (FEEM).

andrea.bastianin@unimi.it

Luca Rossini

University of Milan, Italy and Fondazione Eni Enrico Mattei (FEEM).

luca.rossini@unimi.it

Alessandra Testa

Fondazione Eni Enrico Mattei (FEEM).

January 12, 2026

Contents

A Data description and additional figures

In this section we provide further details about the data used in the paper. As well as additional figures. In particular:

- Table A1 provides details about the data used in the paper.

- Figure A1 shows the data series used in the baseline structural VAR model. The dataset is available from January 1994 to December 2024.

Table A1: Data description

Variable	Description	Source	Transformation	Sample Period
Chile: IP Total	Industrial production: total index	Datastream	$100 * \Delta log$	01-1995:12-2024
Japan: IP Manufacturing	Industrial production: Manufacturing	Datastream	$100 * \Delta log$	01-1995:12-2024
Japan: IP Batteries	Industrial production: Batteries	Datastream	$100 * \Delta log$	01-1995:12-2024
Mexico: IP Total	Industrial production: Total Index	Datastream	$100 * \Delta log$	01-1995:12-2024
IP Total	Industrial production: Total Index	FRED	$100 * \Delta log$	01-1995:12-2024
IP Manufacturing	Industrial production: Manufacturing	FRED	$100 * \Delta log$	01-1995:12-2024
IP Batteries	Industrial production: Battery Manufacturing	FRED	$100 * \Delta log$	01-1995:12-2024
Japan: PPI All Industries	PPI All Industries	METI[a]	$100 * log$	01-1995:12-2022
Japan: PPI Manufacturing	PPI: Total Manufacturing Industries	METI[a]	$100 * log$	01-1995:12-2022
Japan: PPI Mining	PPI: Total Mining	METI[a]	$100 * log$	01-1995:12-2022
PPI All Industries	PPI All Industries	FRED	$100 * log$	01-1995:12-2024
PPI Manufacturing	PPI: Total Manufacturing Industries	FRED	$100 * log$	01-1995:12-2024
PPI Batteries	PPI: Battery Manufacturing	FRED	$100 * log$	01-1995:12-2024
PPI Mining	PPI: Total Mining	FRED	$100 * log$	01-1995:12-2024
Terms of Trade	Terms of trade	Datastream	$100 * log$	01-1995:12-2024
Mexico: Terms of Trade	Terms of trade	Datastream	$100 * log$	01-1995:12-2024
TWEXB	Trade Weighted U.S. Dollar Index: Broad	FRED	$100 * log$	01-1995:12-2019
Chile: REER	Real effective exchange rate	BIS	$100 * log$	01-1995:12-2024
Japan: REER	Real effective exchange rate	BIS	$100 * log$	01-1995:12-2024
Mexico: REER	Real effective exchange rate	BIS	$100 * log$	01-1995:12-2024
REER	Real effective exchange rate	BIS	$100 * log$	01-1995:12-2024

[a] Ministry of Economy, Trade and Industry of Japan Database.

Figure A1: Time series used in the baseline structural VAR model

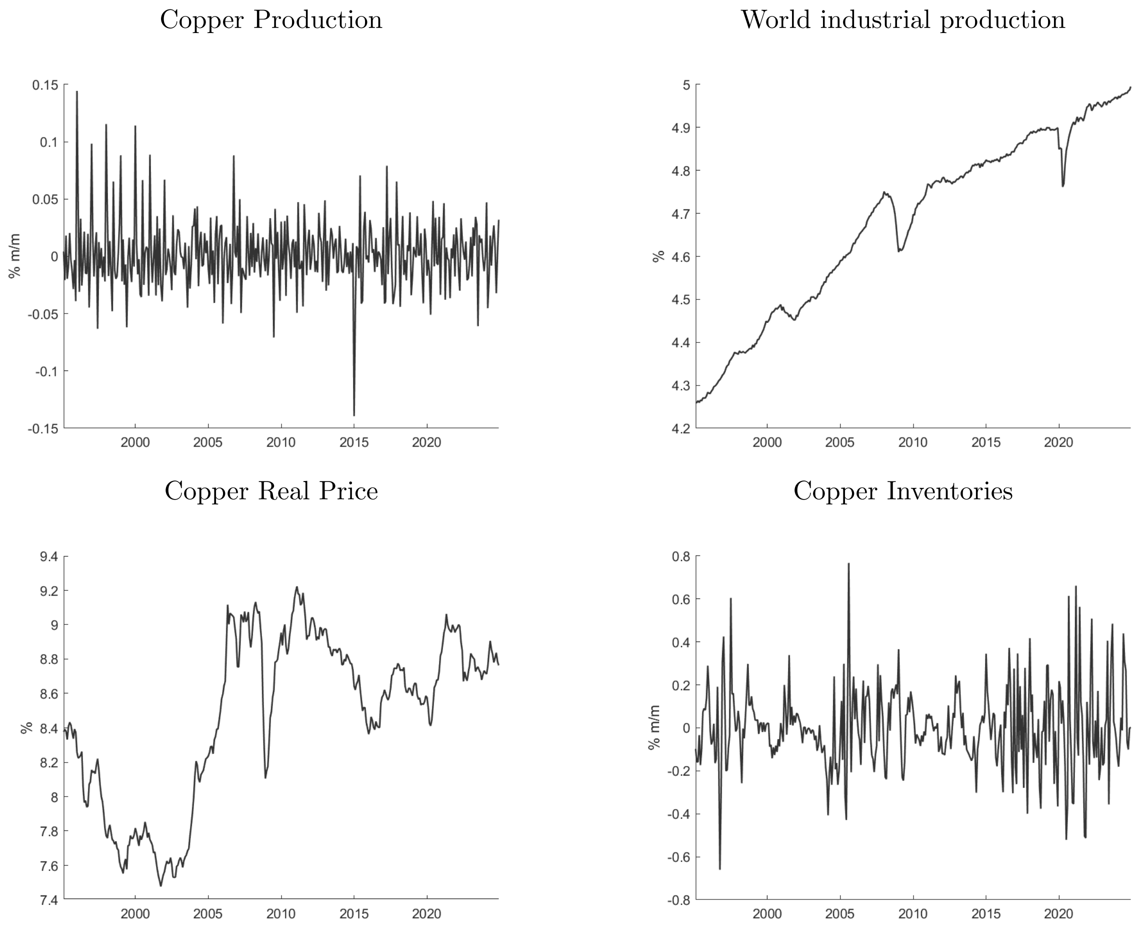

Notes: Time series of the transformed variables over the sample period 1994-2024. Copper production (top-left), its price (bottom left), World industrial production (top right), copper inventories (bottom right).

B VAR analysis: further details and results

The reduced-form VAR is

$$\boldsymbol{y}_t = \sum_{j=1}^{p} \boldsymbol{D}_j \boldsymbol{y}_{t-j} + \boldsymbol{\epsilon}_t \tag{2}$$

where $\boldsymbol{D}_j = \boldsymbol{A}_0^{-1}\boldsymbol{A}_j$ for $j = 1, \ldots, p$. The reduced-form impulse responses satisfy $\boldsymbol{\Phi}_0 = \boldsymbol{I}_n$ and $\boldsymbol{\Phi}_h = \sum_{j=1}^{p} \boldsymbol{D}_j \boldsymbol{\Phi}_{h-j}$ for $h \geq 1$.

Under standard stability conditions, the reduced-form VAR admits the moving-average representation,

$$\boldsymbol{y}_t = \sum_{h=0}^{\infty} \boldsymbol{\Phi}_h \boldsymbol{\epsilon}_{t-h} = \sum_{h=0}^{\infty} \boldsymbol{\Psi}_h \boldsymbol{v}_{t-h}, \tag{3}$$

where $\boldsymbol{\Psi}_h = \boldsymbol{\Phi}_h \boldsymbol{A}_0^{-1}$. The matrices $\{\boldsymbol{\Psi}_h\}_{h=0}^{H}$ define the structural impulse response functions

(IRFs). The (i, j) element of $\mathbf{\Psi}_h$ measures the response of variable i at horizon h to a one-standard-deviation structural shock to variable j at time t.

Additional results. Figure A2 reports the FEVD for copper prices. Figure A3 presents the historical decomposition of the real price of copper around the events considered for the narrative restrictions. Because the exogenous events we identify may affect copper prices both on impact and in the months that follow, the figure shows the average contribution of the supply shock over the month of the event and the subsequent three months. The results indicate that, with the exception of the February 2017 episode, supply shocks played an important role in driving copper price increases around these narrative events.

Figure A2: Forecast error variance decomposition of copper prices

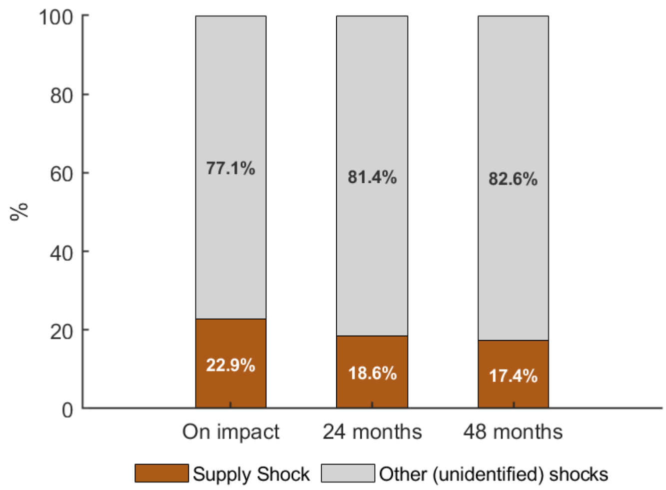

Notes: orange bars represent the share of copper price fluctuations explained by the supply shock, while the gray bars represent the combined contribution of the residual, unidentified shocks.

Figure A3: Historical decomposition around the narrative events

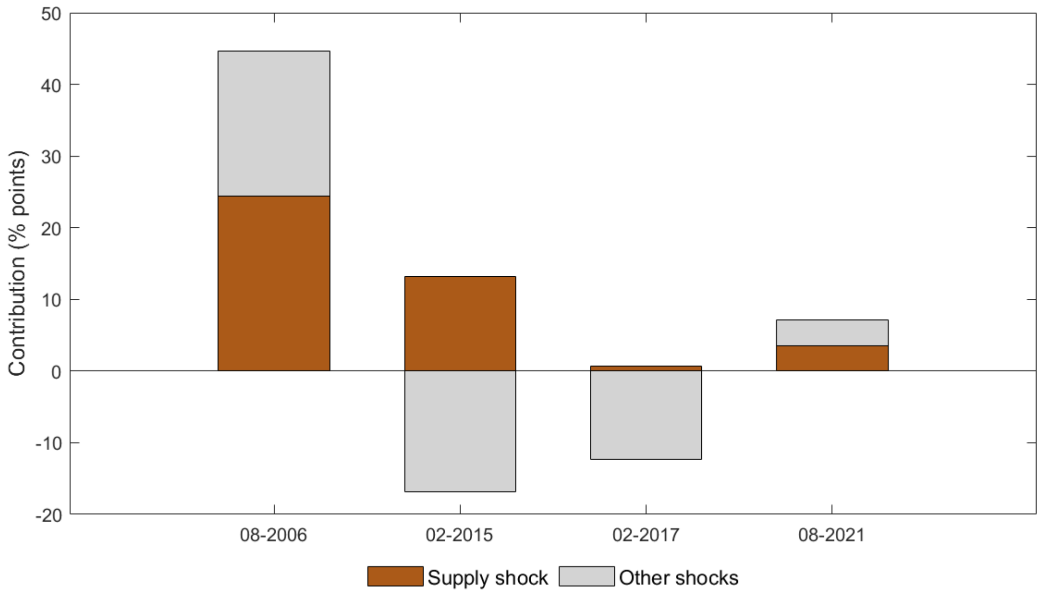

Notes: orange (gray) bars indicate the contribution of (other) supply shocks to the real price of copper around key events.

C Extended robustness checks

C.1 A Structural VAR with additional identified structural shocks

Our baseline model is a four-variable Structural VAR in which we impose restrictions to identify only the copper supply shock, defined as an unexpected decrease in copper production. The literature on supply and demand shocks in commodity markets, such as oil or metals, typically estimates a broader set of structural shocks jointly. Following Boer et al. (2023) we conduct a robustness check in which four shocks are identified – namely, a supply shock, an economic activity shock, a contemporaneous demand shock, and an expectational demand shock – by imposing sign restrictions on the variables in the VAR.

In our case, the algorithm that jointly identifies all shocks using both sign and narrative restrictions does not yield a sufficient number of admissible rotations satisfying the imposed restrictions. For this reason, in this sectione we estimate the four shocks using the sign-restriction scheme proposed by Boer et al. (2024), in order to compare the resulting supply shock and impulse responses with those obtained in our baseline specification.

Inventories are left unrestricted for the supply and economic activity shocks, but are restricted to distinguish between the two demand shocks. Following a contemporaneous demand shock, agents increase copper consumption and draw down inventories in response to higher current demand. By contrast, an expectational demand shock induces agents to accumulate inventories in anticipation of higher future copper demand.

	Production	**IP**	**Price**	**Inventories**
Supply shock	−	−	+	?
Economic activity shock	+	+	+	?
Contemporaneous demand shock	+	−	+	−
Expectational demand shock	+	−	+	+

Table A2: Sign restrictions as in Boer et al. (2024)

Figure A4 compares the time series of the copper supply shock identified using the baseline approach described in Section 4 (black line) with the supply shock obtained from the sign-restriction scheme in Table A2 (red line). The two series display a high degree of similarity, with closely overlapping paths and peaks.

Figure A4: Copper supply shock identified in the partially identified SVAR described in Section 3 (black line) and in the fully identified SVAR using sign restrictions (red line).

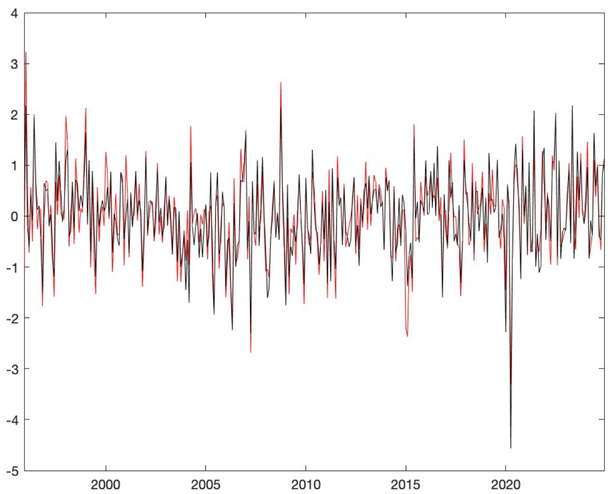

Figure A5 reports the impulse responses to the structural shocks identified according to the restrictions in Table A2. Comparing the first row (impulse responses to the supply shock) with those in Figure **??**, the results are robust in both sign and magnitude relative to our baseline specification. In this alternative model, the price response is somewhat more persistent, remaining positive for over three years following the shock. The response of inventories, when left unrestricted, remains close to zero.

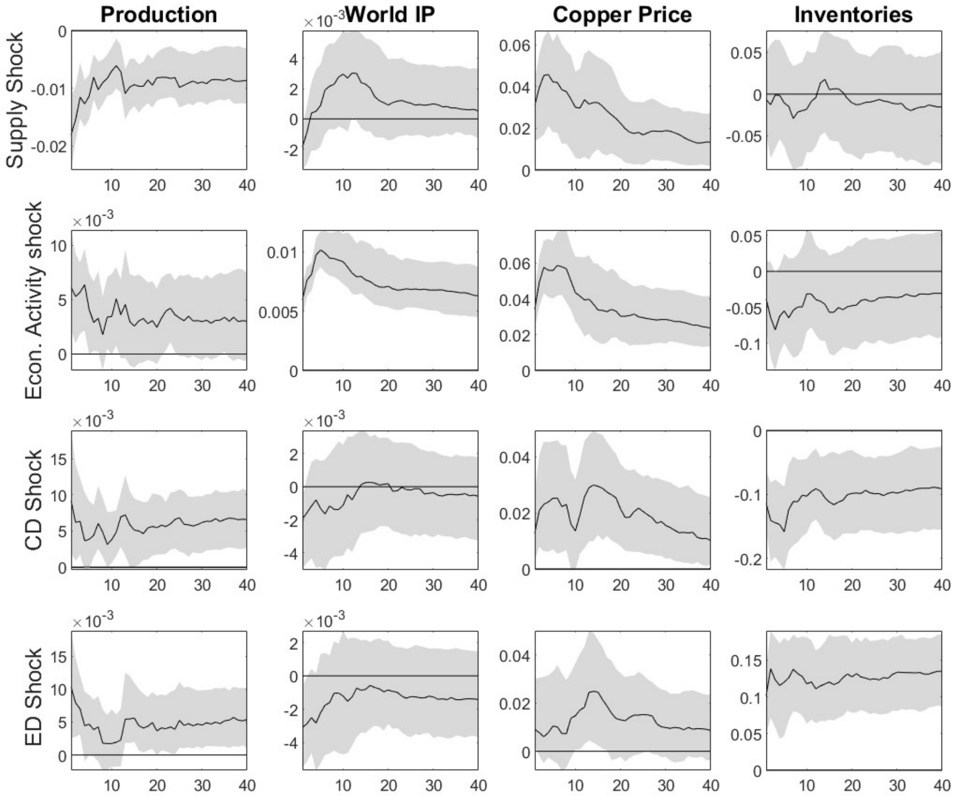

Figure A5: Impulse responses to structural shocks identified following Boer et al. (2024). The IRFs are based on 1,000 draws. The black solid line shows the median response and the gray shaded area represents the 68% pointwise credible set. CD shock denotes the contemporaneous demand shock and ED shock denotes the expectational demand shock.

C.2 The role of refined copper production

As discussed in Section 3, the baseline specification identifies the copper supply shock using mine production. As a robustness check, we also consider an alternative VAR specification that explicitly includes refined copper production, following Boer et al. (2024).

Figure A6 plots the time series of mine production (black line) against refined production (gray line). The latter is defined to include both primary copper – produced via pyrometallurgical routes (smelting concentrates to blister and subsequent electrorefining) or hydrometallurgical routes, notably solvent extraction-electrowinning (SX-EW), which directly yields cathodes from leached copper solutions – and secondary copper, i.e. copper recovered from recycling.

The SVAR model we consider includes five variables: mine production, refined copper production, world industrial production, the real price of copper, and inventories. Global refined copper production data are obtained from the World Bureau of Metal Statistics and are included in the VAR in log-differences. Both production series are de-seasonalized using month-of-the-year dymmy variables.

Figure A6: Copper ore and Refined copper production

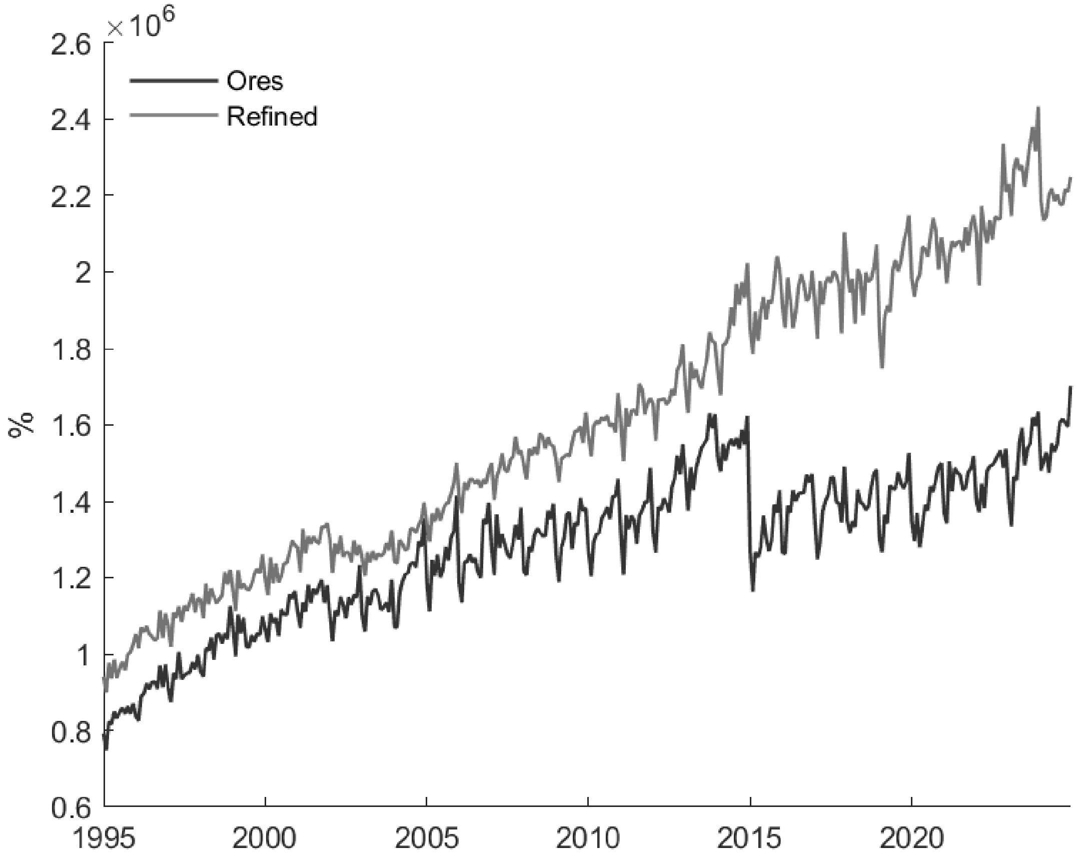

Identification is achieved using the sign restrictions reported in Table A3, together with the narrative restrictions imposed on mine production. Refined copper production is left unrestricted to allow for a flexible response, as its short-run dynamics are not theoretically pinned down, and to avoid over-restricting the system in a way that would substantially reduce the number of admissible rotations.

Figure A7 reports the impulse responses to a negative copper supply shock originating

	Mine Prod.	Refined Prod.	IP	Price	Inventories
Supply shock	−	?	−	+	−

Table A3: Sign restrictions in the five-variable SVAR

in mine production. While the shock has a negative effect on refined copper production, the response is not statistically significant. This muted reaction reflects the presence of lags along the production chain: copper ore is typically converted into concentrate within days or weeks, whereas the transformation from concentrate to refined copper generally requires one to three months—and in some cases longer—due to processing, logistical, and smelting capacity constraints.

A comparison of mine and refined copper production in Figure A6 further illustrates this mechanism. Even after sharp contractions in mine output, refined production does not necessarily decline contemporaneously. A notable example is February 2015, when mine production fell sharply while refined production remained broadly stable. As a result, using refined production in place of mine output would require a different identification strategy, since the narrative restrictions in the baseline specification are anchored to events that directly affected mining operations.

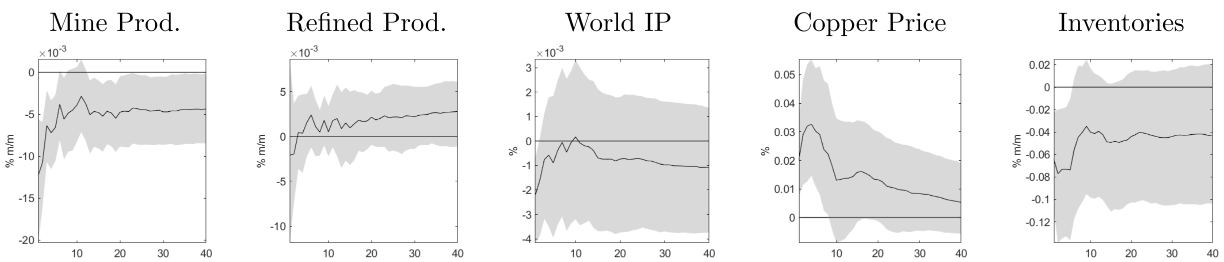

Figure A7: Impulse responses to a negative copper supply shock in the five-variable VAR. The black solid line shows the median response and the gray shaded area represents the 68% pointwise credible set.

C.3 VAR estimation with different lag lengths

In this section, we re-estimate the baseline structural VAR specification using 12 lags instead of 10. The results shown in A8 are qualitatively indistinguishable from those presented in the paper.

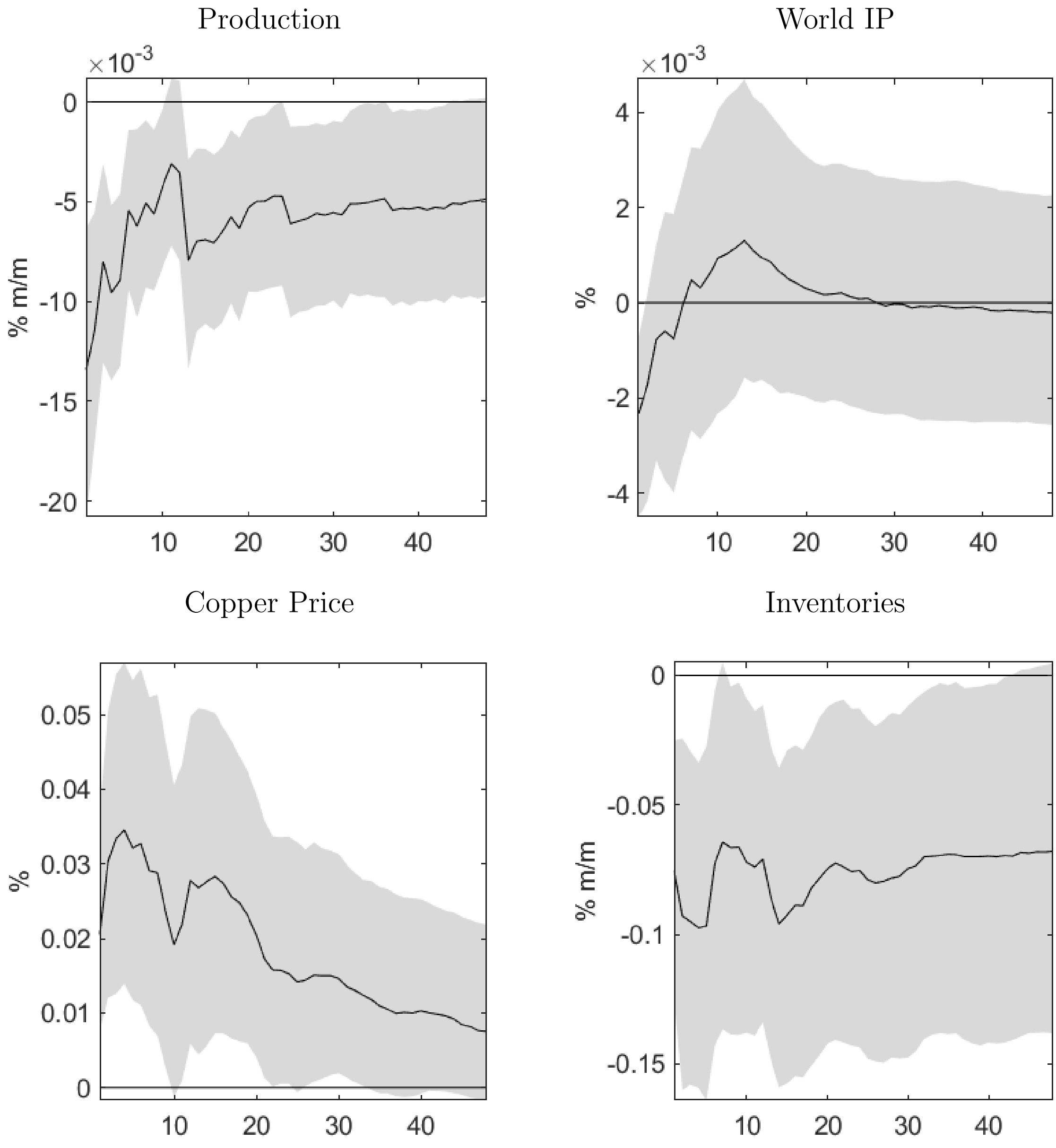

Figure A8: Robustness IRFs with 12 lags to the negative copper supply shock.
The IRFs are based on 1,000 draws. The black solid line shows the median response, the gray shaded area represents the 68% pointwise credible set.

C.4 Estimation of the macroeconomic impact of copper supply shocks with different lag lengths

In this section, we re-estimate the baseline bivariate VAR specifications used to study the transmission channels of copper supply shocks using 12 lags instead of 6. The results are qualitatively indistinguishable from those presented in the paper.

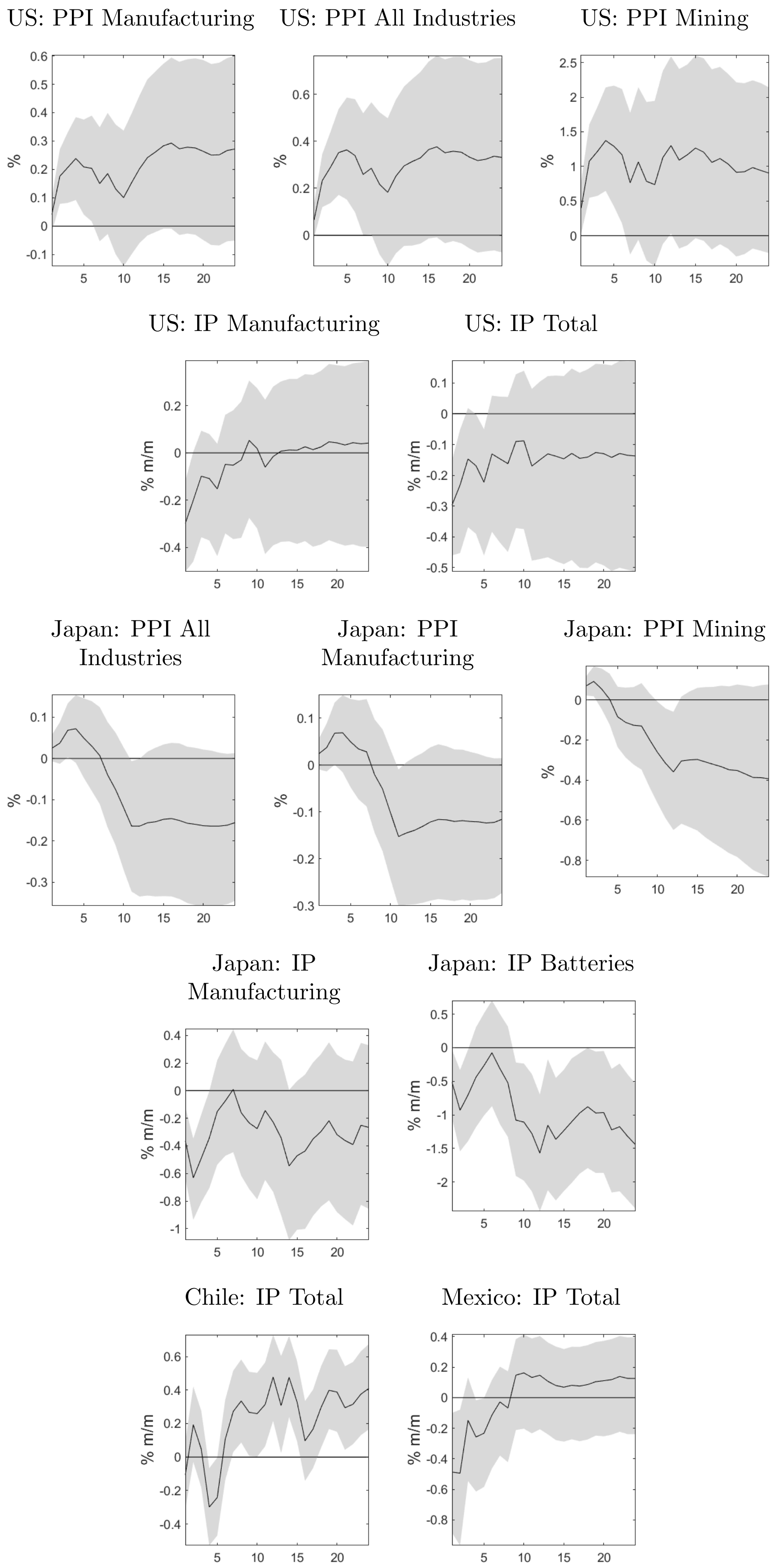

Figure A9: Robustness IRFs with 12 lags for producer price indices (PPI) and industrial production (IP).

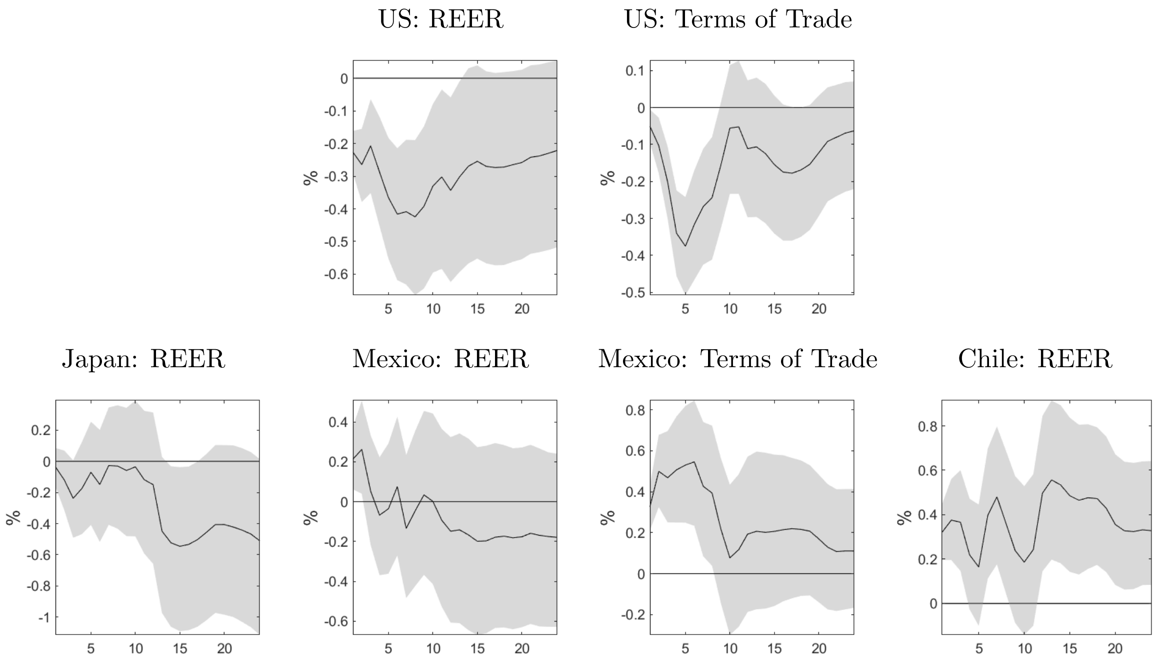

Figure A10: Robustness IRFs with 12 lags for REER, terms of trade. Gray areas show 68% confidence intervals.

C.5 Using all draws of the set-identified shock

In the second step of our empirical strategy, impulse responses are obtained by estimating a bivariate SVAR in which the copper supply shock is ordered first and the macroeconomic variable of interest is ordered second. The copper shock used in this step is recovered from the first stage of the analysis, where it is set-identified rather than point-identified. As a result, the shock is not uniquely determined: instead, the first-step procedure yields a distribution of admissible copper shocks, each associated with a different rotation consistent with the identifying restrictions.

To assess whether the results of the second step depend on a particular draw of the copper supply shock, we conduct a robustness exercise in which we re-estimate the bivariate SVAR using 500 alternative shock draws generated from the identified set. For each draw, we re-estimate the VAR model and compute the impulse response of the variable of interest. These impulse responses are shown in light gray in Figure A11. The solid black line reports the median impulse response across all draws, while the thinner black lines correspond to the 16th and 84th percentiles.

For brevity, we report these robustness impulse responses for two representative variables from the larger set analyzed in the second step. Robustness impulse responses for the remaining variables are reported later in the Supplement. Overall, the impulse response patterns remain stable across all admissible draws of the copper supply shock. This indicates that the results of the second step are not driven by any particular realization of the set-identified shock, and that the median response is highly representative of the full distribution of admissible impulse responses.

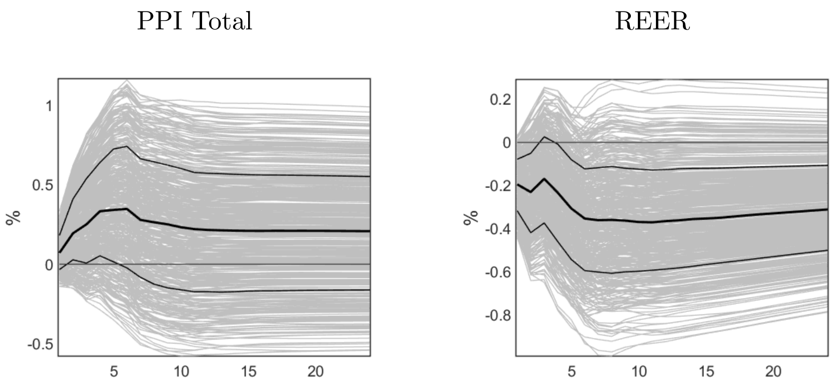

Figure A11: Impulse responses obtained by re-estimating the bivariate SVAR for all admissible draws of the copper supply shock. Each gray line corresponds to the impulse response associated with one draw of the shock. The solid black line reports the median response, while the thin black lines denote the 16th and 84th percentiles.

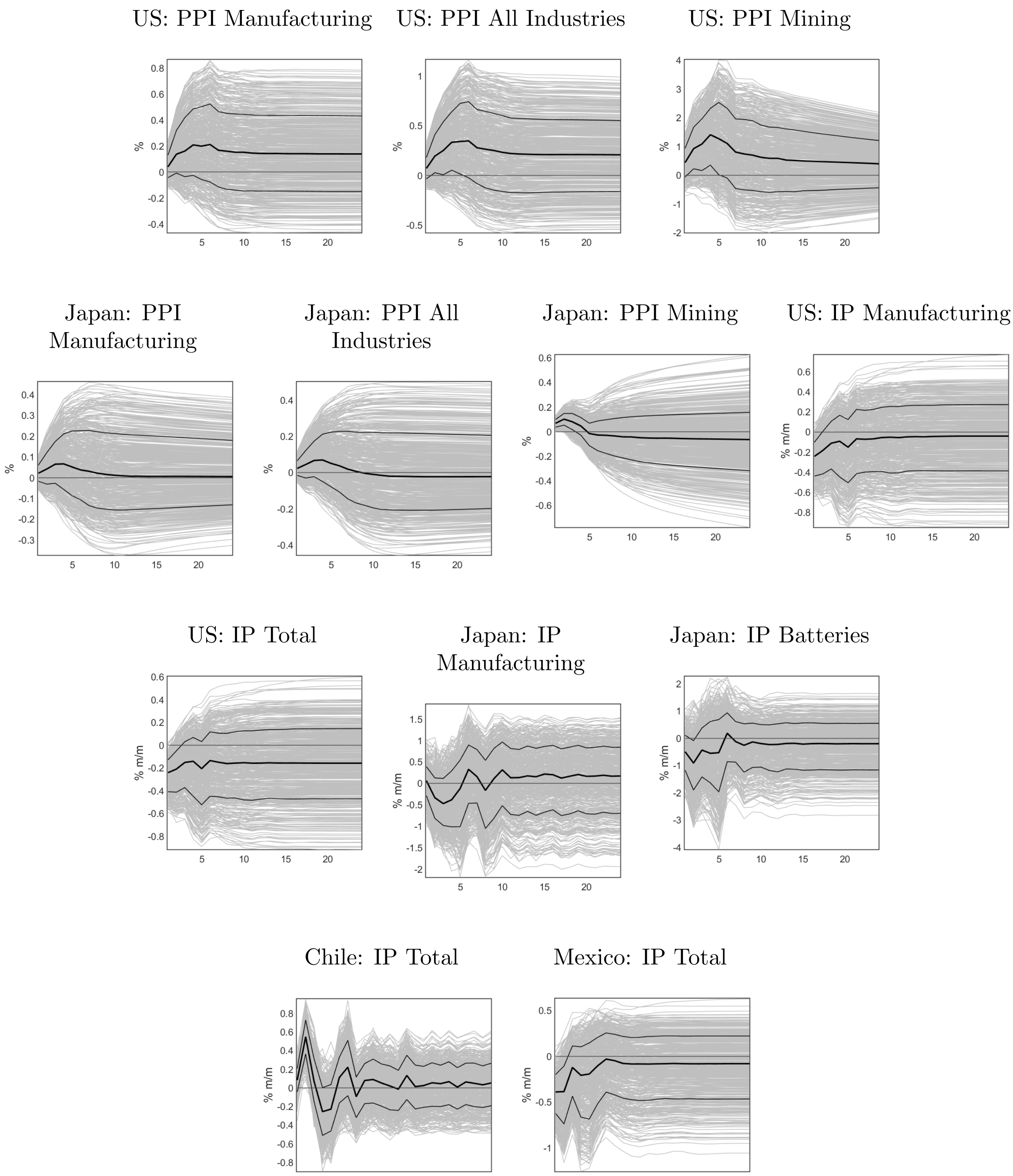

Figure A12: Robustness IRFs with all copper-shock draws for producer price indices (PPI) and industrial production (IP). Gray areas show 68% confidence intervals.

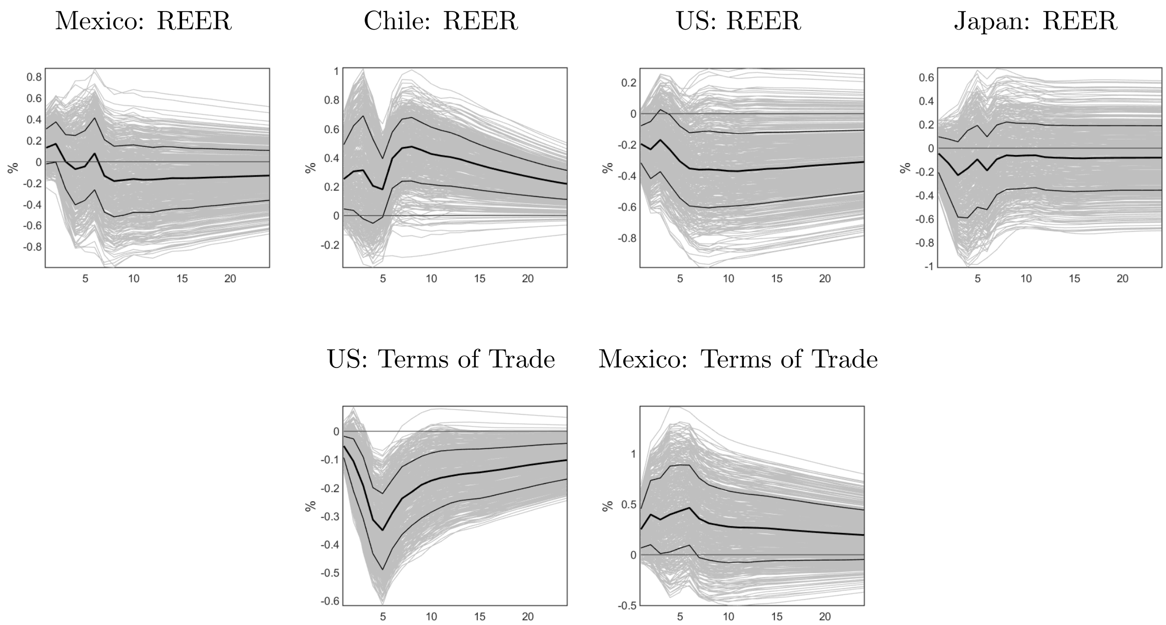

Figure A13: Robustness IRFs with all copper-shock draws for REER, terms of trade. Gray areas show 68% confidence intervals.

C.6 Local projections

In Figures A14, A15 and A16 we compare our baseline SVAR impulse responses with those obtained from local projections (LPs). Specifically, for each horizon $h = 0, \ldots, 24$, we estimate LP impulse responses by regressing y_{t+h} on the identified (median) copper supply shock, controlling for lags of the variables, and computing HAC (Newey–West) standard errors.

Figure A14: Local projections – US

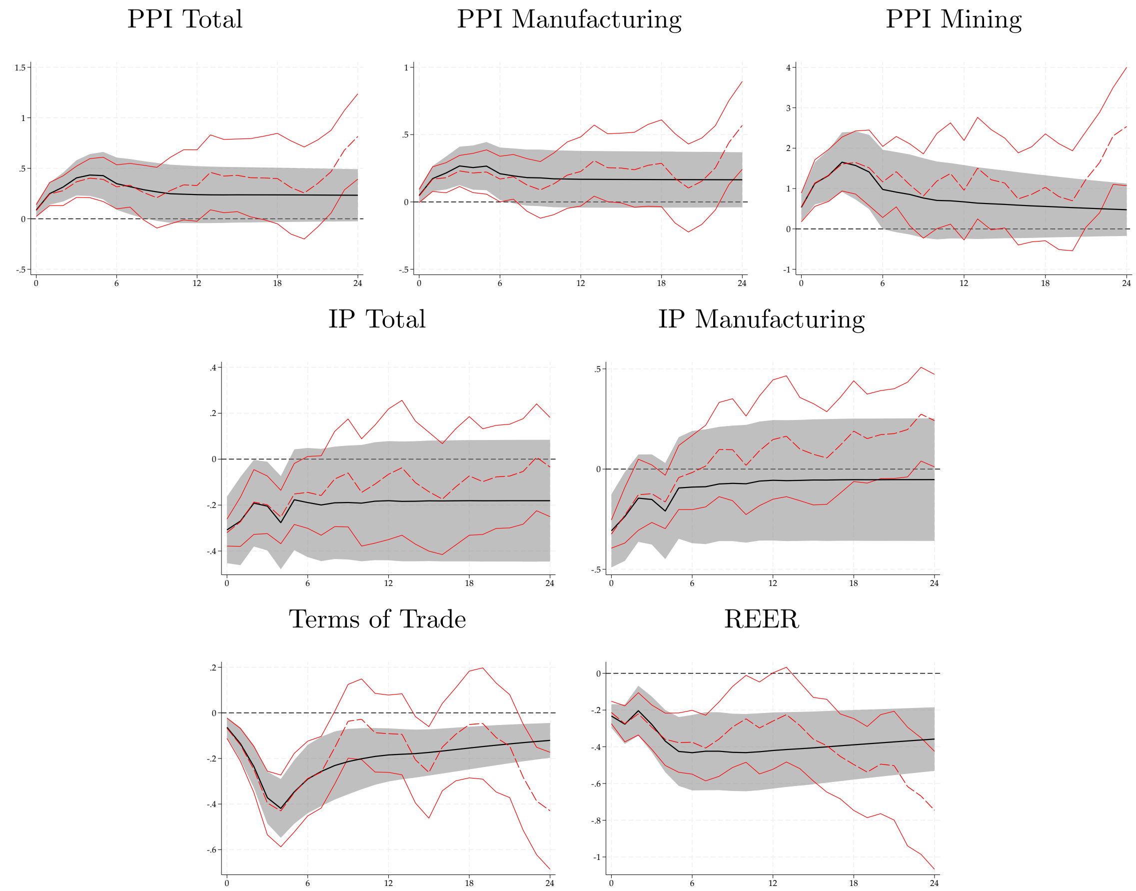

Notes: Gray shaded areas represent 68% confidence bands based on 5,000 bootstrap replications. In all specifications, the response variable is expressed as 100 times the logarithm of the underlying series. The sole exception is industrial production (IP), which enters the model in 100 times log differences; for these specifications, impulse responses are reported in cumulative form. Black solid lines represent the SVAR-based IRFs. Red dashed lines denote the corresponding LP-based IRFs, while red solid lines represent the associated 68% confidence bands based on HAC standard errors.

Figure A15: LP IRFs for Japan.

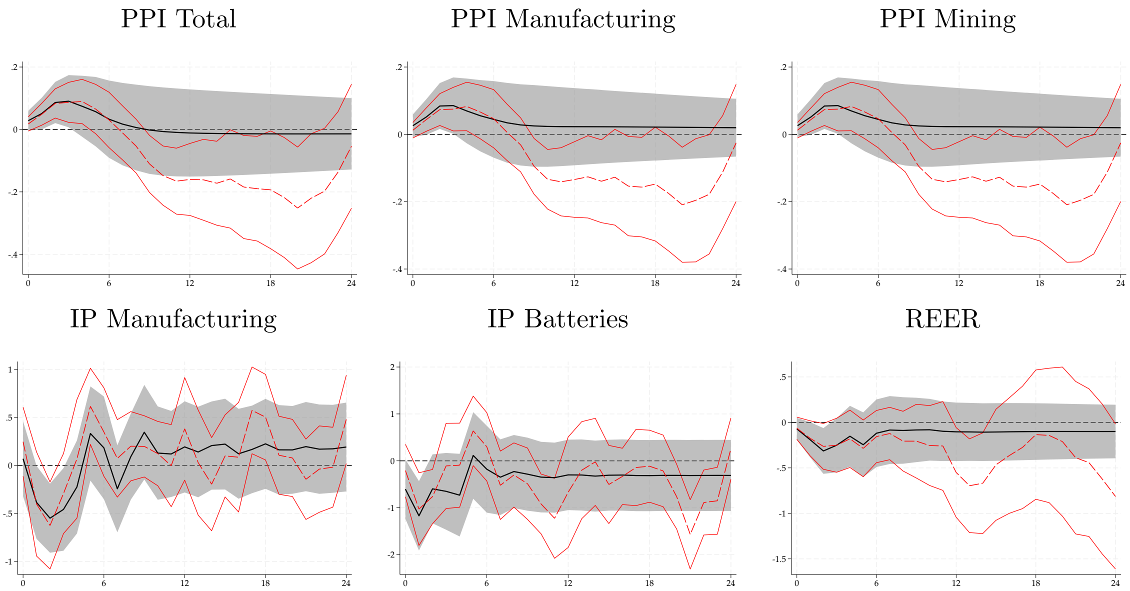

Notes: see notes to Figure A14.

Figure A16: LP IRFs for Chile and Mexico.

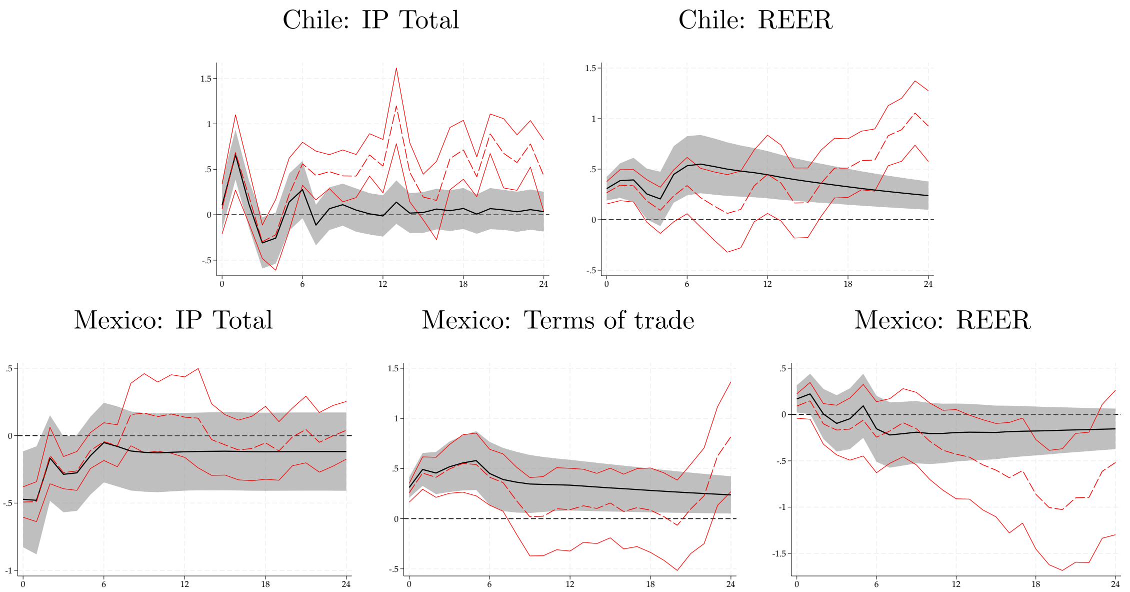

Notes: see notes to Figure A14.

FONDAZIONE ENI ENRICO MATTEI WORKING PAPER SERIES

Our Working Papers are available on the Internet at the following address:
https://www.feem.it/pubblicazioni/feem-working-papers/

"NOTE DI LAVORO" PUBLISHED IN 2026

1. R. Corbi, C. Falco, L. J. Uberti, Dams and Rural Conflict: Evidence from Brazil's Hydropower Expansion

Fondazione Eni Enrico Mattei
Corso Magenta 63, Milano – Italia

Tel. +39 02 403 36934

E-mail: letter@feem.it
www.feem.it